

Finite Temperature Field Theory and Phase Transitions*

Mariano Quirós

Instituto de Estructura de la Materia (CSIC), Serrano 123
E-28006 Madrid, Spain

Abstract

We review different aspects of field theory at zero and finite temperature, related to the theory of phase transitions. We discuss different renormalization conditions for the effective potential at zero temperature, emphasizing in particular the $\overline{\text{MS}}$ renormalization scheme. Finite temperature field theory is discussed in the real and imaginary time formalisms, showing their equivalence in simple examples. Bubble nucleation by thermal tunneling, and the subsequent development of the phase transition is described in some detail. Some attention is also devoted to the breakdown of the perturbative expansion and the infrared problem in the finite temperature field theory. Finally the application to baryogenesis at the electroweak phase transition is done in the Standard Model and in the Minimal Supersymmetric Standard Model. In all cases we have translated the condition of not washing out any previously generated baryon asymmetry by upper bounds on the Higgs mass.

IEM-FT-187/99
January 1999

*Based on lectures given at the *Summer School in High Energy Physics and Cosmology*, ICTP, Trieste (Italy) 29 June–17 July 1998.

1 The effective potential at zero temperature

The effective potential for quantum field theories was originally introduced by Euler, Heisenberg and Schwinger¹, and applied to studies of spontaneous symmetry breaking by Goldstone, Salam, Weinberg and Jona-Lasinio². Calculations of the effective potential were initially performed at one-loop by Coleman and E. Weinberg³ and at higher-loop by Jackiw⁴ and Iliopoulos, Itzykson and Martin⁵. More recently the effective potential has been the subject of a vivid investigation, especially related to its invariance under the renormalization group. I will try to review, in this section, the main ideas and update the latest developments on the effective potential.

1.1 Generating functionals

To fix the ideas, let us consider the theory described by a scalar field ϕ with a lagrangian density $\mathcal{L}\{\phi(x)\}$ and an action

$$S[\phi] = \int d^4x \mathcal{L}\{\phi(x)\} \quad (1)$$

The generating functional (vacuum-to-vacuum amplitude) is given by the path-integral representation,

$$Z[j] = \langle 0_{\text{out}} | 0_{\text{in}} \rangle_j \equiv \int d\phi \exp\{i(S[\phi] + \phi j)\} \quad (2)$$

where we are using the notation

$$\phi j \equiv \int d^4x \phi(x) j(x) \quad (3)$$

Using (2) one can obtain the connected generating functional $W[j]$ defined as,

$$Z[j] \equiv \exp\{iW[j]\} \quad (4)$$

and the effective action $\Gamma[\bar{\phi}]$ as the Legendre transform of (4)

$$\Gamma[\bar{\phi}] = W[j] - \int d^4x \frac{\delta W[j]}{\delta j(x)} j(x) \quad (5)$$

where

$$\bar{\phi}(x) = \frac{\delta W[j]}{\delta j(x)} \quad (6)$$

In particular, from (5) and (6), the following equality can be easily proven,

$$\frac{\delta\Gamma[\bar{\phi}]}{\delta\bar{\phi}} = \frac{\delta W[j]}{\delta j} \frac{\delta j}{\delta\bar{\phi}} - j - \bar{\phi} \frac{\delta j}{\delta\bar{\phi}} = -j \quad (7)$$

where we have made use of the notation (3). Eq. (7) implies in particular that,

$$\left. \frac{\delta\Gamma[\bar{\phi}]}{\delta\bar{\phi}} \right|_{j=0} = 0 \quad (8)$$

which defines de vacuum of the theory in the absence of external sources.

We can now expand $Z[j]$ ($W[j]$) in a power series of j , to obtain its representation in terms of Green functions $G_{(n)}$ (connected Green functions $G_{(n)}^c$) as,

$$Z[j] = \sum_{n=0}^{\infty} \frac{i^n}{n!} \int d^4x_1 \dots d^4x_n j(x_1) \dots j(x_n) G_{(n)}(x_1, \dots, x_n) \quad (9)$$

and

$$iW[j] = \sum_{n=0}^{\infty} \frac{i^n}{n!} \int d^4x_1 \dots d^4x_n j(x_1) \dots j(x_n) G_{(n)}^c(x_1, \dots, x_n) \quad (10)$$

Similarly the effective action can be expanded in powers of $\bar{\phi}$ as

$$\Gamma[\bar{\phi}] = \sum_{n=0}^{\infty} \frac{1}{n!} \int d^4x_1 \dots d^4x_n \bar{\phi}(x_1) \dots \bar{\phi}(x_n) \Gamma^{(n)}(x_1, \dots, x_n) \quad (11)$$

where $\Gamma^{(n)}$ are the one-particle irreducible (1PI) Green functions.

We can Fourier transform $\Gamma^{(n)}$ and $\bar{\phi}$ as,

$$\Gamma^{(n)}(x) = \int \prod_{i=1}^n \left[\frac{d^4p_i}{(2\pi)^4} \exp\{ip_i x_i\} \right] (2\pi)^4 \delta^{(4)}(p_1 + \dots + p_n) \Gamma^{(n)}(p) \quad (12)$$

$$\tilde{\phi}(p) = \int d^4x e^{-ipx} \bar{\phi}(x) \quad (13)$$

and obtain for (5) the expression,

$$\Gamma[\bar{\phi}] = \sum_{n=0}^{\infty} \int \prod_{i=1}^n \left[\frac{d^4p_i}{(2\pi)^4} \tilde{\phi}(-p_i) \right] (2\pi)^4 \delta^{(4)}(p_1 + \dots + p_n) \Gamma^{(n)}(p_1, \dots, p_n) \quad (14)$$

In a translationally invariant theory,

$$\bar{\phi}(x) = \phi_c \quad (15)$$

the field $\bar{\phi}$ is constant. Removing an overall factor of space-time volume, we define the effective potential $V_{\text{eff}}(\phi_c)$ as,

$$\Gamma[\phi_c] = - \int d^4x V_{\text{eff}}(\phi_c) \quad (16)$$

Using now the definition of Dirac δ -function,

$$\delta^{(4)}(p) = \int \frac{d^4x}{(2\pi)^4} e^{-ipx} \quad (17)$$

and (15) in (13) we obtain,

$$\tilde{\phi}_c(p) = (2\pi)^4 \phi_c \delta^{(4)}(p). \quad (18)$$

Replacing (18) in (14) we can write the effective action for constant field configurations as,

$$\Gamma(\phi_c) = \sum_{n=0}^{\infty} \frac{1}{n!} \phi_c^n (2\pi)^4 \delta^{(4)}(0) \Gamma^{(n)}(p_i = 0) = \sum_{n=0}^{\infty} \frac{1}{n!} \phi_c^n \Gamma^{(n)}(p_i = 0) \int d^4x \quad (19)$$

and comparing it with (16) we obtain the final expression,

$$V_{\text{eff}}(\phi_c) = - \sum_{n=0}^{\infty} \frac{1}{n!} \phi_c^n \Gamma^{(n)}(p_i = 0) \quad (20)$$

which will be used for explicit calculations of the effective potential.

Let us finally mention that there is an alternative way of expanding the effective action: it can also be expanded in powers of momentum, about the point where all external momenta vanish. In configuration space that expansion reads as:

$$\Gamma[\bar{\phi}] = \int d^4x \left[-V_{\text{eff}}(\bar{\phi}) + \frac{1}{2} (\partial_\mu \bar{\phi}(x))^2 Z(\bar{\phi}) + \dots \right] \quad (21)$$

1.2 The one-loop effective potential

We are now ready to compute the effective potential. In particular the zero-loop contribution is simply the classical (tree-level) potential. The one-loop contribution is readily computed using the previous techniques and can be written in closed form for any field theory containing spinless particles, spin- $\frac{1}{2}$ fermions and gauge bosons. Here we will follow closely the calculation of Ref.³.

Scalar fields

We consider the simplest model of one self-interacting real scalar field, described by the lagrangian

$$\mathcal{L} = \frac{1}{2} \partial^\mu \phi \partial_\mu \phi - V_0(\phi) \quad (22)$$

with a tree-level potential

$$V_0 = \frac{1}{2} m^2 \phi^2 + \frac{\lambda}{4!} \phi^4 \quad (23)$$

The one-loop correction to the tree-level potential should be computed as the sum of all 1PI diagrams with a single loop and zero external momenta. Diagrammatically they are displayed in Fig. 1, where each vertex has 2 external legs.

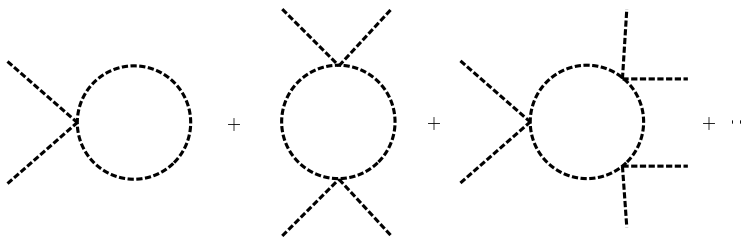


Figure 1: 1PI diagrams contributing to the one-loop effective potential of (22).

The n -th diagram has n propagators, n vertices and $2n$ external legs. The n propagators will contribute a factor of $i^n (p^2 - m^2 + i\epsilon)^{-n}$ ^a. The external lines contribute a factor of ϕ_c^{2n} and each vertex a factor of $-i\lambda/2$, where the factor $1/2$ comes from the fact that interchanging the 2 external lines of the vertex does not change the diagram. There is a global symmetry factor $\frac{1}{2n}$, where $\frac{1}{n}$ comes from the symmetry of the diagram under the discrete group of rotations \mathbf{Z}_n and $\frac{1}{2}$ from the symmetry of the diagram under reflection. Finally there is an integration over the loop momentum and an extra global factor of i from the definition of the generating functional.

Using the previous rules the one-loop effective potential can be computed as,

$$V_{\text{eff}}(\phi_c) = V_0(\phi_c) + V_1(\phi_c),$$

^aWe are using the Bjorken and Drell's⁶ notation and conventions.

with

$$\begin{aligned}
V_1(\phi_c) &= i \sum_{n=1}^{\infty} \int \frac{d^4 p}{(2\pi)^4} \frac{1}{2n} \left[\frac{\lambda \phi_c^2/2}{p^2 - m^2 + i\epsilon} \right]^n \\
&= -\frac{i}{2} \int \frac{d^4 p}{(2\pi)^4} \log \left[1 - \frac{\lambda \phi_c^2/2}{p^2 - m^2 + i\epsilon} \right]
\end{aligned} \tag{24}$$

After a Wick rotation

$$p^0 = ip_E^0, \quad p_E = (-ip^0, \vec{p}), \quad p^2 = (p^0)^2 - \vec{p}^2 = -p_E^2, \tag{25}$$

Eq. (24) can be cast as,

$$V_1(\phi_c) = \frac{1}{2} \int \frac{d^4 p_E}{(2\pi)^4} \log \left[1 + \frac{\lambda \phi_c^2/2}{p_E^2 + m^2} \right] \tag{26}$$

Finally, using the *shifted* mass

$$m^2(\phi_c) = m^2 + \frac{1}{2} \lambda \phi_c^2 = \frac{d^2 V_0(\phi_c)}{d\phi_c^2} \tag{27}$$

and dropping the subindex E from the euclidean momenta, we can write the final expression of the one-loop contribution to the effective potential as,

$$V_1(\phi_c) = \frac{1}{2} \int \frac{d^4 p}{(2\pi)^4} \log [p^2 + m^2(\phi_c)] \tag{28}$$

where a field independent term has been neglected.

The result of Eq. (28) can be trivially generalized to the case of N_s **complex** scalar fields described by the lagrangian,

$$\mathcal{L} = \partial^\mu \phi^a \partial_\mu \phi_a^\dagger - V_0(\phi^a, \phi_a^\dagger). \tag{29}$$

The one-loop contribution to the effective potential in the theory described by the lagrangian (29) is given by

$$V_1 = \frac{1}{2} Tr \int \frac{d^4 p}{(2\pi)^4} \log [p^2 + M_s^2(\phi^a, \phi_b^\dagger)] \tag{30}$$

where

$$(M_s^2)_b^a \equiv V_b^a = \frac{\partial^2 V}{\partial \phi_a^\dagger \partial \phi^b} \tag{31}$$

and $Tr M_s^2 = 2 V_a^a$, where the factor of 2 comes from the fact that each complex field contains two degrees of freedom. Similarly $Tr \mathbf{1} = 2 N_s$.

Fermion fields

We consider now a theory with fermion fields described by the lagrangian,

$$\mathcal{L} = i\bar{\psi}_a \gamma \cdot \partial \psi^a - \bar{\psi}_a (M_f)_b^a \psi^b \quad (32)$$

where the mass matrix $(M_f)_b^a(\phi_c^i)$ is a function of the scalar fields linear in ϕ_c^i : $(M_f)_b^a = \Gamma_{bi}^a \phi_c^i$.

The diagrams contributing to the one-loop effective potential are depicted in Fig. 2.

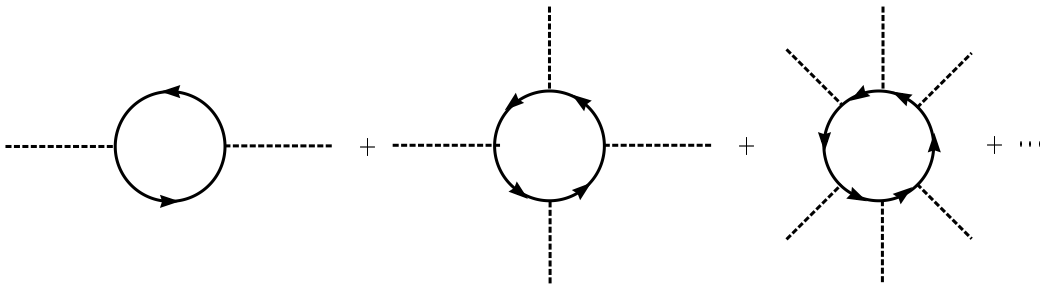


Figure 2: 1PI diagrams contributing to the one-loop effective potential of (32).

Diagrams with an odd number of vertices are zero because of the γ -matrices property: $tr(\gamma^{\mu_1} \dots \gamma^{\mu_{2n+1}}) = 0$. The diagram with $2n$ vertices has $2n$ fermionic propagators. The propagators yield a factor

$$Tr_s [i^{2n} (\gamma \cdot p)^{2n} (p^2 + i\epsilon)^{-2n}]$$

where Tr_s refers to spinor indices. The vertices contribute as

$$Tr [-i^{2n} M_f(\phi_c)^{2n}]$$

where Tr runs over the different fermionic fields. There is also a combinatorial factor $\frac{1}{2n}$ (from the cyclic and anticyclic symmetry of diagrams) and an overall -1 coming from the fermions loop. One finally obtains the total factor

$$-\frac{1}{2n} \frac{Tr(M_f^{2n})}{p^{2n}} \cdot Tr_s \mathbf{1}.$$

The factor $Tr_s \mathbf{1}$ just counts the number of degrees of freedom of the fermions. It is equal to 4 if Dirac fermions are used, and 2 if Weyl fermions (and σ -matrices) are present. So we will write,

$$Tr_s \mathbf{1} = 2\lambda \quad (33)$$

where $\lambda = 1$ ($\lambda = 2$) for Weyl (Dirac) fermions. On the other hand we have grouped terms pairwise in the matrix product and used,

$$\tilde{p}^2 = p^2$$

where \tilde{p} stands either for $p \cdot \gamma$ or $p \cdot \sigma$, depending on the kind of fermions we are using.

Collecting everything together we can write the one-loop contribution to the effective potential from fermion fields as,

$$V_1(\phi_c) = -2\lambda i \text{Tr} \sum_{n=1}^{\infty} \int \frac{d^4 p}{(2\pi)^4} \frac{1}{2n} \left[\frac{M_f^2}{p^2} \right]^n = 2\lambda \frac{i}{2} \text{Tr} \int \frac{d^4 p}{(2\pi)^4} \log \left[1 - \frac{M_f^2}{p^2} \right] \quad (34)$$

As in the case of the scalar theory, after making a Wick rotation to the Euclidean momenta space, and neglecting an irrelevant field independent term, we can cast (34) as

$$V_1 = -2\lambda \frac{1}{2} \text{Tr} \int \frac{d^4 p}{(2\pi)^4} \log [p^2 + M_f^2(\phi_c)] \quad (35)$$

Gauge bosons

Consider now a theory described by the lagrangian,

$$\mathcal{L} = -\frac{1}{4} \text{Tr}(F_{\mu\nu} F^{\mu\nu}) + \frac{1}{2} \text{Tr}(D_\mu \phi_a)^\dagger D^\mu \phi^a + \dots \quad (36)$$

In the Landau gauge, which does not require ghost-compensating terms, the free gauge-boson propagator is

$$\Pi_\nu^\mu = -\frac{i}{p^2 + i\epsilon} \Delta_\nu^\mu \quad (37)$$

with

$$\Delta_\nu^\mu = g_\nu^\mu - \frac{p^\mu p_\nu}{p^2} \quad (38)$$

satisfying the property $p_\mu \Delta_\nu^\mu = 0$ and $\Delta^n = \Delta$, $n = 1, 2, \dots$

The only vertex which contributes to one-loop is

$$\mathcal{L} = \frac{1}{2} (M_{gb})_{\alpha\beta}^2 A_\mu^\alpha A^{\mu\beta} + \dots \quad (39)$$

where

$$(M_{gb})_{\alpha\beta}^2(\phi_c) = g_\alpha g_\beta \text{Tr} \left[(T_{\alpha\ell}^i \phi_i)^\dagger T_{\beta j}^\ell \phi^j \right] \quad (40)$$

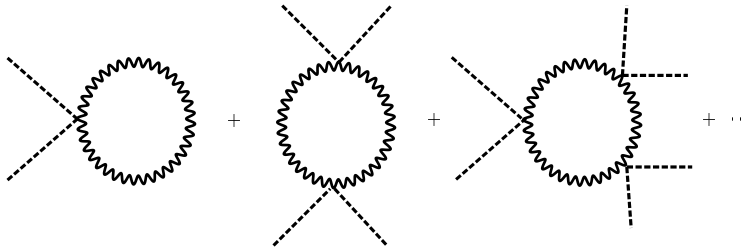


Figure 3: 1PI diagrams contributing to the one-loop effective potential of (36).

In this way the diagrams contributing to the one-loop effective potential are depicted in Fig. 3.

A few comments about Eq. (40): **(i)** g_α is the gauge coupling constant associated to the gauge field A_μ^α ; if the gauge group is simple, *e.g.* $SU(5)$, $SO(10)$, E_6, \dots , then all gauge couplings are equal; otherwise there is a distinct gauge coupling per group factor. **(ii)** T_α are the generators of the Lie algebra of the gauge group in the representation of the ϕ -fields and the trace in (40) is over indices of that representation.

Taking into account the combinatorial factors, the graph with n propagators and n vertices yields a total factor

$$\frac{1}{2n} \frac{Tr((M_{gb})^2)^n}{p^{2n}} Tr(\Delta)$$

where

$$Tr(\Delta) = 3 \tag{41}$$

which is the number of degrees of freedom of a massive gauge boson. Collecting together all factors, and making the Wick rotation to the euclidean momenta space, we can cast the effective potential from gauge bosons as,

$$V_1 = Tr(\Delta) \frac{1}{2} Tr \int \frac{d^4 p}{(2\pi)^4} \log [p^2 + (M_{gb})^2(\phi_c)] \tag{42}$$

1.3 The higher-loop effective potential

Calculating the effective potential by summing infinite series of Feynman graphs at zero external momentum is an extremely onerous task beyond the one-loop approximation. However, as has been shown in Ref. ⁴, this task is trivial for

the case of one-loop, and affordable for the case of higher-loop. Here we will just summarize the result of Ref. ^{4 b}.

We will start considering the theory described by a real scalar field, with a lagrangian \mathcal{L} given in (22-23), and an action as in (1). We will define another lagrangian $\hat{\mathcal{L}}$ by the following procedure:

$$\int d^4x \hat{\mathcal{L}}\{\phi_c; \phi(x)\} \equiv S[\phi_c + \phi] - S[\phi_c] - \phi \frac{\delta S[\phi_c]}{\delta \phi_c} \quad (43)$$

where we have used in the last term the notation (3). In (43), ϕ_c is an x -independent shifting field. The second term in (43) makes the vacuum energy equal to zero, and the third term is there to cancel the tadpole part of the shifted action.

If we denote by $\mathcal{D}\{\phi_c; x - y\}$ the propagator of the shifted theory,

$$i\mathcal{D}^{-1}\{\phi_c; x - y\} = \left. \frac{\delta^2 S[\phi]}{\delta \phi(x) \delta \phi(y)} \right|_{\phi=\phi_c} \quad (44)$$

and

$$i\mathcal{D}^{-1}\{\phi_c; p\}$$

its Fourier transform, the effective potential is found to be given by ⁴:

$$\begin{aligned} V_{\text{eff}}(\phi_c) &= V_0(\phi_c) - \frac{i}{2} \int \frac{d^4p}{(2\pi)^4} \log \det i\mathcal{D}^{-1}\{\phi_c; p\} \\ &+ i \left\langle \exp \left[i \int d^4x \hat{\mathcal{L}}_I\{\phi_c; \phi(x)\} \right] \right\rangle \end{aligned} \quad (45)$$

The first term in (45) is just the classical tree-level potential. The second term is the one-loop potential, where the determinant operates on any possible internal indices defining the propagator. The third term summarizes the following operation: Compute all 1PI vacuum diagrams, with conventional Feynman rules, using the propagator of the shifted theory $\mathcal{D}\{\phi_c; p\}$ and the interaction provided by the interaction lagrangian $\hat{\mathcal{L}}_I\{\phi_c; \phi(x)\}$, and delete the overall factor of space-time volume $\int d^4x$ from the effective action (16). It can be shown that the last term in (45) starts at two-loop. Every term in (45) resums an infinite number of Feynman diagrams of the unshifted theory.

In the simple example of the lagrangian (22-23) it can be easily seen that the shifted potential is given by

$$\hat{V}\{\phi_c; \phi\} = \frac{1}{2} m^2(\phi_c) \phi^2 + \frac{\lambda}{3!} \phi_c \phi^3 + \frac{\lambda}{4!} \phi^4 \quad (46)$$

^bThe interested reader can find in ⁴ all calculational details.

where the shifted mass is defined in (27). The shifted propagator is found to be

$$i\mathcal{D}^{-1}\{\phi_c; p\} = p^2 - m^2(\phi_c) \quad (47)$$

and the second term of (45) easily computed to be

$$V_1(\phi_c) = -\frac{i}{2} \int \frac{d^4 p}{(2\pi)^4} \log[p^2 - m^2(\phi_c)] \quad (48)$$

which is easily seen to coincide with (24), up to field independent terms, so that after the Wick rotation we recover the result (28).

The two-loop effective potential is harder than the one-loop term, but affordable. The result can be found in Ref. ⁴. Diagrammatically, the one- and two-loop effective potentials are given by the “figure-eight” plus the “sunset” diagrams, where it is understood that we are using the Feynman rules of the shifted theory, as stated above.

Of course, the previous rules apply also to theories containing fermions and gauge bosons. The Feynman rules of the shifted theory applied to all 1PI diagrams provide the total effective potential according to (45). In particular it is trivial to obtain the one-loop effective potential for fermions and gauge bosons, as given by Eqs. (35) and (42), respectively. Notice that the masses $M_f^2(\phi_c)$, in (35), and $M_{gb}^2(\phi_c)$, in (42) are the masses in the corresponding shifted theories. Diagrammatically (35) and (42) can be represented in the shifted theory as vacuum diagrams with one fermion and one gauge boson loop, respectively.

1.4 Renormalizations conditions

The final expression of the effective potential we have deduced in the previous section, Eqs. (28), (35) and (42), is ultraviolet-divergent. To make sense out of it we have to follow the renormalization procedure of quantum field theories. First of all, to give a sense to the ultraviolet behaviour of the theory we have to make it finite: *i.e.* we have to **regularize** the theory. Second of all, all infinities have to be absorbed by appropriate **counterterms**, which were not explicitly written in our previous expressions. The way these infinities are absorbed by the counterterms depend on the definition of the **renormalized parameters**, *i.e.* on the choice of the **renormalization conditions**. Finally the theory, written as a function of the renormalized parameters, is finite.

In this way, the first step towards renormalizing the theory is choosing the regularization scheme. We will first present the straightforward regularization using a cut-off of momenta.

Cut-off regularization

We will illustrate this scheme with the simplest theory: a massless real scalar field, with a lagrangian

$$\mathcal{L} = \frac{1}{2}(1 + \delta Z)(\partial_\mu \phi)^2 - \frac{1}{2}\delta m^2 \phi^2 - \frac{\lambda + \delta\lambda}{4!}\phi^4 \quad (49)$$

where δZ , δm^2 and $\delta\lambda$ are the usual wave-function, mass and coupling constant renormalization counterterms. They have to be defined self-consistently order by order in the loop expansion. Here we will compute everything to one-loop order.

The conventional definition of the renormalized mass of the scalar field is the negative inverse propagator at zero momentum. In view of (20) we can write it as:

$$m_R^2 = -\Gamma^{(2)}(p=0) = \left. \frac{d^2 V}{d\phi_c^2} \right|_{\phi_c=0} \quad (50)$$

We can also define the renormalized coupling as the four-point function at zero external momentum,

$$\lambda_R = -\Gamma^{(4)}(p=0) = \left. \frac{d^4 V}{d\phi_c^4} \right|_{\phi_c=0} \quad (51)$$

and the standard condition for the field renormalization is,

$$Z(0) = 1 \quad (52)$$

Now we will compute the effective potential (28) cutting off the integral at $p^2 = \Lambda^2$. First of all we can integrate over angular variables. For that we can use,

$$\int d^n p f(\rho) = \frac{\pi^{n/2}}{\Gamma(\frac{n}{2})} \int f(\rho) \rho^{n/2-1} d\rho \quad (53)$$

where $\rho = |p|^2$, and we can cast (28) as

$$V_1(\phi_c) = \frac{1}{32\pi^2} \int_0^{\Lambda^2} \rho \log[\rho + m^2(\phi_c)] d\rho. \quad (54)$$

This indefinite integral can be solved with the help of⁷

$$\int x \log(a+x) dx = \frac{1}{2}(x^2 - a^2) \log(a+x) - \frac{1}{2} \left(\frac{x^2}{2} - ax \right)$$

Neglecting now in (54) field independent terms, and terms which vanish in the limit $\Lambda \rightarrow \infty$, we finally obtain,

$$V_1(\phi_c) = \frac{1}{32\pi^2} m^2(\phi_c) \Lambda^2 + \frac{1}{64\pi^2} m^4(\phi_c) \left[\log \frac{m^2(\phi_c)}{\Lambda^2} - \frac{1}{2} \right] \quad (55)$$

Using now (55) we can write the one-loop effective potential of the theory (49) as,

$$V = \frac{1}{2} \delta m^2 \phi_c^2 + \frac{\lambda + \delta\lambda}{4!} \phi_c^4 + \frac{\lambda \phi_c^2}{64\pi^2} \Lambda^2 + \frac{\lambda^2 \phi_c^4}{256\pi^2} \left(\log \frac{\lambda \phi_c^2}{2\Lambda^2} - \frac{1}{2} \right) \quad (56)$$

We will impose now a variant of the renormalization conditions (50), (51) and (52). For the renormalized mass we can impose it to vanish, *i.e.*,

$$\left. \frac{d^2 V}{d\phi_c^2} \right|_{\phi_c=0} = 0 \quad (57)$$

For the renormalized gauge coupling λ , we cannot use Eq. (51) at a value of the field equal to zero. There is nothing wrong with using a different renormalization prescription and using a different subtraction point. We can use,

$$\lambda = \left. \frac{d^4 V}{d\phi_c^4} \right|_{\phi_c=\mu} \quad (58)$$

where μ is some mass scale. Different choices of the scale lead to different definitions of the coupling constant, *i.e.* to different parametrizations of the same theory, but in principle any value of μ is as good as any other.

Imposing now the conditions (57) and (58) to (56) we can write the counterterms as,

$$\delta m^2 = -\frac{\lambda}{32\pi^2} \Lambda^2 \quad (59)$$

and

$$\delta\lambda = -\frac{11\lambda^2}{32\pi^2} - \frac{3\lambda^2}{32\pi^2} \log \frac{\lambda\mu^2}{2\Lambda^2} \quad (60)$$

Using now (59) and (60) in (56) we can write the one-loop effective potential in the previous renormalization scheme as,

$$V_{\text{eff}} = \frac{\lambda}{4!} \phi_c^4 + \frac{\lambda^2 \phi_c^4}{256\pi^2} \log \left(\frac{\phi_c^2}{\mu^2} - \frac{25}{6} \right) \quad (61)$$

A similar renormalization scheme can be defined also for theories with fermions and/or gauge bosons. However for gauge theories the regularization

provided by the cut-off explicitly break gauge invariance so that the dimensional regularization is better suited for them. In the next section we will review the calculation of the effective potential in the dimensional regularization and define the so-called $\overline{\text{MS}}$ scheme.

Dimensional regularization

This regularization scheme was introduced by t'Hooft and Veltman⁸. It consists in making an analytic continuation of Feynman integrals to the complex plane in the number of space-time dimensions n . The integrals have singularities which arise as poles in $1/(n-4)$ and have to be subtracted out. The particular prescription for subtraction is called a **renormalization scheme**. In working with the effective potential it is customary to use the so-called $\overline{\text{MS}}$ renormalization scheme⁹.

We will compute now the one-loop effective potential (28) using dimensional regularization, *i.e.*

$$V_1(\phi_c) = \frac{1}{2}(\mu^2)^{2-\frac{n}{2}} \int \frac{d^n p}{(2\pi)^n} \log [p^2 + m^2(\phi_c)] \quad (62)$$

where μ is a scale with mass dimension which needs to be introduced to balance the dimension of the integration measure. It is simpler to compute the tadpole

$$V' = \frac{1}{2}(\mu^2)^{2-\frac{n}{2}} \int \frac{d^n p}{(2\pi)^n} \frac{1}{p^2 + m^2(\phi_c)} \quad (63)$$

where the meaning of V' is the derivative with respect to $m^2(\phi_c)$, using the basic formula of dimensional regularization,

$$\int d^n p \frac{(p^2)^\alpha}{(p^2 + M^2)^\beta} = \pi^{\frac{n}{2}} (M^2)^{\frac{n}{2} + \alpha - \beta} \frac{\Gamma(\alpha + \frac{n}{2}) \Gamma(\beta - \alpha - \frac{n}{2})}{\Gamma(\frac{n}{2}) \Gamma(\beta)} \quad (64)$$

and integrating the resulting integral with respect to $m^2(\phi_c)$. One can then write the regularized potential (62) as,

$$V_1(\phi_c) = -\frac{1}{32\pi^2} \frac{1}{\frac{n}{2}(\frac{n}{2}-1)} \left(\frac{m^2(\phi_c)}{4\pi\mu^2} \right)^{\frac{n}{2}-2} \Gamma\left(2 - \frac{n}{2}\right) m^4(\phi_c) \quad (65)$$

We can expand (65) in powers of $2 - n/2$ and use the expansion

$$\Gamma(z) = \frac{1}{z} - \gamma_E + \mathcal{O}(z) \quad (66)$$

where $\gamma_E = 0.5772\dots$ is the Euler-Mascheroni constant⁷. We obtain for (65)

$$V_1(\phi_c) = \frac{m^4(\phi_c)}{64\pi^2} \left\{ - \left[\frac{1}{2 - \frac{n}{2}} - \gamma_E + \log 4\pi \right] + \log \frac{m^2(\phi_c)}{\mu^2} - \frac{3}{2} + \mathcal{O}\left(\frac{n}{2} - 2\right) \right\} \quad (67)$$

Now the $\overline{\text{MS}}$ renormalization scheme consists in subtracting the term proportional to

$$C_{\text{UV}} \equiv \left[\frac{1}{2 - \frac{n}{2}} - \gamma_E + \log 4\pi \right] \quad (68)$$

in the regularized potential (67). Therefore the divergent piece,

$$-\frac{m^4(\phi_c)}{64\pi^2} \left\{ \left[\frac{1}{2 - \frac{n}{2}} - \gamma_E + \log 4\pi \right] \right\}$$

has to be absorbed by the counterterms. Therefore the final expression for the one-loop potential, written in terms of the renormalized parameters, is

$$V_1(\phi_c) = \frac{1}{64\pi^2} m^4(\phi_c) \left\{ \log \frac{m^2(\phi_c)}{\mu^2} - \frac{3}{2} \right\} \quad (69)$$

For instance, in the theory described by lagrangian (49), the counterterms are given by,

$$\begin{aligned} \delta m^2 &= 0 \\ \delta \lambda &= \frac{3\lambda^2}{32\pi^2} \left[\frac{1}{2 - \frac{n}{2}} - \gamma_E + \log 4\pi \right] \end{aligned} \quad (70)$$

and the effective potential is,

$$V_{\text{eff}} = \frac{\lambda}{4!} \phi_c^4 + \frac{\lambda^2 \phi_c^4}{256\pi^2} \log \left(\frac{\lambda \phi_c^2}{2\mu^2} - \frac{3}{2} \right) \quad (71)$$

The scale μ along this section is related to the renormalization group behaviour of the renormalized couplings and masses.

For a theory with fermion fields, one needs a trace operation in dimensional regularization, as $\text{Tr} \mathbf{1} = f(n)$. For instance, for an even dimension one could choose, $f(n) = 2^{n/2}$ for Dirac fermions, and $f(n) = 2^{n/2-1}$ for Weyl fermions. However the difference $f(n) - f(4)$ is only relevant for divergent graphs and can therefore be absorbed by a renormalization-group transformation. It is

usually convenient to choose $f(n) = f(4) = 2\lambda$ for all values of n ¹⁰. The effective potential (35) can be computed as in (62), leading to,

$$V_1(\phi_c) = -\lambda \frac{M_f^4(\phi_c)}{32\pi^2} \left\{ - \left[\frac{1}{2 - \frac{n}{2}} - \gamma_E + \log 4\pi \right] + \log \frac{M_f^2(\phi_c)}{\mu^2} - \frac{3}{2} + \mathcal{O}\left(\frac{n}{2} - 2\right) \right\} \quad (72)$$

In the $\overline{\text{MS}}$ renormalization scheme, after subtracting the term proportional to (68) we obtain,

$$V_1(\phi_c) = -\lambda \frac{1}{32\pi^2} M_f^4(\phi_c) \left\{ \log \frac{M_f^2(\phi_c)}{\mu^2} - \frac{3}{2} \right\} \quad (73)$$

Similarly, in a theory with gauge bosons as in (36), the effective potential (42) is computed as,

$$V_1(\phi_c) = Tr(\Delta) \frac{M_{gb}^4(\phi_c)}{64\pi^2} \left\{ - \left[\frac{1}{2 - \frac{n}{2}} - \gamma_E + \log 4\pi \right] + \log \frac{M_{gb}^2(\phi_c)}{\mu^2} - \frac{3}{2} + \mathcal{O}\left(\frac{n}{2} - 2\right) \right\} \quad (74)$$

where

$$Tr(\Delta) = n - 1 \quad (75)$$

In the $\overline{\text{MS}}$ renormalization scheme, subtracting as usual the term proportional to (68) one obtains the effective potential,

$$V_1(\phi_c) = 3 \frac{1}{64\pi^2} M_{gb}^4(\phi_c) \left\{ \log \frac{M_{gb}^2(\phi_c)}{\mu^2} - \frac{5}{6} \right\} \quad (76)$$

A variant of the $\overline{\text{MS}}$ renormalization scheme is the $\overline{\text{DR}}$ renormalization scheme¹¹, where the dimensional regularization is applied only to the scalar part of the integrals, while all fermion and tensor indices are considered in four dimensions. In this case $Tr(\Delta)$ is taken equal to 3, as in (41), and subtracting from (74) the term proportional to (68) one obtains,

$$V_1(\phi_c) = 3 \frac{1}{64\pi^2} M_{gb}^4(\phi_c) \left\{ \log \frac{M_{gb}^2(\phi_c)}{\mu^2} - \frac{3}{2} \right\} \quad (77)$$

1.5 One-loop effective potential for the Standard Model

In this subsection we will apply the above ideas to compute the one loop effective potential for the Standard Model of electroweak interactions. The spin-zero fields of the Standard Model are described by the $SU(2)$ doublet,

$$\Phi = \left(\begin{array}{c} \chi_1 + i\chi_2 \\ \frac{\phi_c + h + i\chi_3}{\sqrt{2}} \end{array} \right) \quad (78)$$

where ϕ_c is the real constant background, h the Higgs field, and χ_a ($a=1,2,3$) are the three Goldstone bosons. The tree level potential reads, in terms of the background field, as

$$V_0(\phi_c) = -\frac{m^2}{2}\phi_c^2 + \frac{\lambda}{4}\phi_c^4 \quad (79)$$

with positive λ and m^2 , and the tree level minimum corresponding to

$$v^2 = \frac{m^2}{\lambda}.$$

The spin-zero field dependent masses are

$$\begin{aligned} m_h^2(\phi_c) &= 3\lambda\phi_c^2 - m^2 \\ m_\chi^2(\phi_c) &= \lambda\phi_c^2 - m^2 \end{aligned} \quad (80)$$

so that $m_h^2(v) = 2\lambda v^2 = 2m^2$ and $m_\chi^2(v) = 0$. The gauge bosons contributing to the one-loop effective potential are W^\pm and Z , with tree level field dependent masses,

$$\begin{aligned} m_W^2(\phi_c) &= \frac{g^2}{4}\phi_c^2 \\ m_Z^2(\phi_c) &= \frac{g^2 + g'^2}{4}\phi_c^2 \end{aligned} \quad (81)$$

Finally, the only fermion which can give a significant contribution to the one loop effective potential is the top quark, with a field-dependent mass

$$m_t^2(\phi_c) = \frac{h_t^2}{2}\phi_c^2 \quad (82)$$

where h_t is the top quark Yukawa coupling.

The one-loop effective potential $V_1(\phi_c)$ can be computed using Eqs. (28), (35) and (42). As we have said in the previous subsection, these integrals are

ultraviolet divergent. They have to be regularized and the divergent contributions cancelled by the counterterms

$$V_1^{\text{c.t.}} = \delta\Omega + \frac{\delta m^2}{2}\phi_c^2 + \frac{\delta\lambda}{4}\phi_c^4 \quad (83)$$

where we have introduced a counterterm $\delta\Omega$ for the vacuum energy or cosmological constant (see next section).

The final expression for the effective potential is finite and depends on the used regularization and, correspondingly, on the renormalization conditions. Next we will describe the two most commonly used renormalization conditions for the Standard Model.

$\overline{\text{MS}}$ renormalization

In this case we can use Eqs. (67), (72) and (74) for the contribution to $V_1(\phi_c)$ of the scalars, fermions and gauge bosons, respectively. In the $\overline{\text{MS}}$ renormalization scheme we subtract the terms proportional to C_{UV} , see Eq. (68), which are cancelled by the counterterms in (83). One easily arrives to the finite effective potential provided by

$$V(\phi_c) = V_0(\phi_c) + \frac{1}{64\pi^2} \sum_{i=W,Z,h,\chi,t} n_i m_i^4(\phi_c) \left[\log \frac{m_i^2(\phi_c)}{\mu^2} - C_i \right] \quad (84)$$

where C_i are constants given by,

$$\begin{aligned} C_W = C_Z &= \frac{5}{6} \\ C_h = C_\chi = C_t &= \frac{3}{2} \end{aligned} \quad (85)$$

and n_i are the degrees of freedom

$$n_W = 6, \quad n_Z = 3, \quad n_h = 1, \quad n_\chi = 3, \quad n_t = -12 \quad (86)$$

The counterterms which cancel the infinities are provided by,

$$\begin{aligned} \delta\Omega &= \frac{m^4}{64\pi^2} (n_h + n_\chi) C_{\text{UV}} \\ \delta m^2 &= -\frac{3\lambda m^2}{16\pi^2} \left(n_h + \frac{1}{3}n_\chi \right) C_{\text{UV}} \\ \delta\lambda &= \frac{3}{16\pi^2} \left[\frac{2g^4 + (g^2 + g'^2)^2}{16} - h_t^4 + \left(3n_h + \frac{1}{3}n_\chi \right) \lambda^2 \right] C_{\text{UV}} \end{aligned} \quad (87)$$

where C_{UV} is defined in (68). We have explicitly written in (87) the contribution to the counterterms from the Higgs sector, n_h and n_χ . The latter give rise entirely to the mass counterterms δm^2 and $\delta\Omega$. For Higgs masses lighter than W masses, the Higgs sector can be ignored in the one loop radiative corrections (as it is usually done) and the massive counterterms are not generated.

Cut-off regularization

A very useful scheme¹² is obtained by regularizing the theory with a cut-off and imposing that the minimum, at $v = 246.22 \text{ GeV}$, and the Higgs mass does not change with respect to their tree level values, *i.e.*,

$$\begin{aligned} \left. \frac{d(V_1 + V_1^{c.t.})}{d\phi_c} \right|_{\phi_c=v} &= 0 \\ \left. \frac{d^2(V_1 + V_1^{c.t.})}{d\phi_c^2} \right|_{\phi_c=v} &= 0 \end{aligned} \quad (88)$$

Now we can use (55) to write

$$V_1(\phi_c) = \frac{1}{32\pi^2} \sum_{i=W,Z,t,h,\chi} n_i \left[m_i^2(\phi_c)\Lambda^2 + \frac{m_i^4(\phi_c)}{2} \left(\log \frac{m_i^2(\phi_c)}{\Lambda^2} - \frac{1}{2} \right) \right] \quad (89)$$

Imposing now the conditions (88) the infinities in (89) cancel against those in $V_1^{c.t.}$, and the resulting ϕ_c -dependent potential is finite, and given by,

$$V(\phi_c) = V_0(\phi_c) + \frac{1}{64\pi^2} \sum_i \left\{ m_i^4(\phi_c) \left(\log \frac{m_i^2(\phi_c)}{m_i^2(v)} - \frac{3}{2} \right) + 2m_i^2(v)m_i^2(\phi_c) \right\} \quad (90)$$

The counterterms $\delta\Omega$, δm^2 and $\delta\lambda$ in (83) turn out to be given by

$$\begin{aligned} \delta\lambda &= -\frac{1}{16\pi^2} \sum_i n_i \left(\frac{m_i^2(v) - b_i}{v^2} \right)^2 \left(\log \frac{m_i^2(v)}{\Lambda^2} + 1 \right) \\ \delta m^2 &= -\frac{1}{16\pi^2} \sum_i n_i \frac{m_i^2 - b_i}{v^2} \left[\Lambda^2 - m_i^2(v) + b_i \left(\log \frac{m_i^2(v)}{\Lambda^2} + 1 \right) \right] \\ \delta\Omega &= \frac{m^2}{32\pi^2} \sum_{i=h,\chi} n_i \left[\Lambda^2 - m_i^2(v) + \frac{1}{2} b_i \left(\log \frac{m_i^2(v)}{\Lambda^2} + 1 \right) \right] \end{aligned} \quad (91)$$

where $b_W = b_Z = b_t = 0$ and $b_h = b_\chi = -m^2$.

We can see again in (91) that ignoring the contribution to the one loop effective potential from the Higgs sector results in the non appearance of a cosmological constant. However, unlike the $\overline{\text{MS}}$ scheme, δm^2 is also generated by the contribution of the gauge boson and top quark loops. Of course the one loop counterterms we are computing along this section are only useful for two loop calculations.

1.6 Improved effective potential and renormalization group

As we have seen in the previous section, the calculation of the effective action involves a mass μ which is not physical in the sense that all the theory should be independent of the chosen value of μ . In fact a change in μ should be accompanied by a change in the renormalized parameters (couplings and masses) such that all the theory remains unchanged. This statement for the effective action can be expressed as an equation³

$$\left[\mu \frac{\partial}{\partial \mu} + \beta_i \frac{\partial}{\partial \lambda_i} - \gamma \phi_c \frac{\delta}{\delta \phi_c} \right] \Gamma[\phi_c] = 0 \quad (92)$$

for an appropriate choice of the coefficients β_i and γ , where λ_i denotes collectively all couplings and masses of the theory. In the last term of (92) we have made use of the notation (3).

We define the effective potential \hat{V} as in Eq. (20),

$$\hat{V} \equiv \hat{V}(\mu, \lambda_i, \phi_c) = \hat{V}(\mu, \lambda_i, 0) - \sum_{n=1}^{\infty} \frac{1}{n!} \phi_c^n \Gamma^{(n)}(p_i = 0) \quad (93)$$

The role of the vacuum energy $\hat{\Omega}$,

$$\hat{\Omega} = \hat{V}(\mu, \lambda_i, 0)$$

has been recently stressed in Ref. ¹³. Using now the renormalization group equation (RGE) satisfied by the effective action (92), we obtain the RGE satisfied by \hat{V} as

$$\left[\mu \frac{\partial}{\partial \mu} + \beta_i \frac{\partial}{\partial \lambda_i} - \gamma \phi_c \frac{\partial}{\partial \phi_c} \right] \hat{V} = \left[\mu \frac{\partial}{\partial \mu} + \beta_i \frac{\partial}{\partial \lambda_i} \right] \hat{\Omega} \quad (94)$$

If we make a ϕ_c -independent shift to \hat{V} such that,

$$\begin{aligned} V &= \hat{V} + \Delta \hat{\Omega}(\mu, \lambda_i) \\ \Omega &\equiv \hat{\Omega} + \Delta \hat{\Omega} \end{aligned} \quad (95)$$

with the condition,

$$\left[\mu \frac{\partial}{\partial \mu} + \beta_i \frac{\partial}{\partial \lambda_i} \right] \Omega = 0 \quad (96)$$

then the potential V satisfies the well known RGE,

$$\left[\mu \frac{\partial}{\partial \mu} + \beta_i \frac{\partial}{\partial \lambda_i} - \gamma \phi_c \frac{\partial}{\partial \phi_c} \right] V = 0 \quad (97)$$

The formal solutions to Eqs. (96) and (97) can be written as,

$$\begin{aligned} V &\equiv V(\mu, \lambda_i, \phi_c) = V(\mu(t), \lambda_i(t), \phi(t)) \\ \Omega &\equiv \Omega(\mu, \lambda_i) = \Omega(\mu(t), \lambda_i(t)) \end{aligned} \quad (98)$$

where

$$\begin{aligned} \mu(t) &= \mu \exp(t) \\ \phi(t) &= \phi_c \xi(t) \\ \xi(t) &= \exp \left\{ - \int_0^t \gamma(\lambda_i(t')) dt' \right\} \\ \beta_i(\lambda(t)) &= \frac{d\lambda_i(t)}{dt} \end{aligned} \quad (99)$$

with the boundary conditions,

$$\begin{aligned} \mu(0) &= \mu \\ \phi(0) &= \phi_c \\ \xi(0) &= 1 \\ \lambda_i(0) &= \lambda_i \end{aligned} \quad (100)$$

In fact Eqs. (96) and (97) can be simply written as,

$$\begin{aligned} \frac{d}{dt} \Omega &= 0 \\ \frac{d}{dt} V &= 0 \end{aligned} \quad (101)$$

which state that Ω and V are scale-independent. Of course the same happens to all derivatives of V ,

$$V^{(n)}(\mu, \lambda_i, \phi_c) \equiv \frac{\partial^n V(\mu, \lambda_i, \phi_c)}{\partial \phi_c^n} \quad (102)$$

which by virtue of (99) satisfies

$$V^{(n)} = \xi(t)^n \frac{\partial^n}{\partial \phi(t)^n} V(\mu(t), \lambda_i(t), \phi(t)) \quad (103)$$

The RGE satisfied by $V^{(n)}$ can be obtained from (97) and the property,

$$\frac{\partial^n}{\partial \phi_c^n} \left[-\gamma \phi_c \frac{\partial}{\partial \phi_c} \right] = \left[-\gamma \phi_c \frac{\partial}{\partial \phi_c} \right] \frac{\partial^n}{\partial \phi_c^n} - n\gamma \frac{\partial^n}{\partial \phi_c^n}$$

It is given by,

$$\left[\mu \frac{\partial}{\partial \mu} + \beta_i \frac{\partial}{\partial \lambda_i} - \gamma \phi_c \frac{\partial}{\partial \phi_c} \right] V^{(n)} = n\gamma V^{(n)} \quad (104)$$

which implies that $V^{(n)}$ is scale independent.

In particular the scale independence of $V^{(n)}$, $n = 0, 1, \dots$, means that we can fix the scale t at any value, even ϕ_c -dependent. Suppose we fix t by the arbitrary conditions,

$$\begin{aligned} \mu(t) &= f(\phi_c) \\ t = t(\phi_c) &= \log\{f(\phi_c)/\mu\} \\ \phi(t) &= \xi(t(\phi_c))\phi_c \end{aligned} \quad (105)$$

Using (105) we can write the effective potential and its derivatives (102) as ϕ_c -functions,

$$V(\phi_c) \equiv V[f(\phi_c), \lambda_i(t(\phi_c)), \phi(t(\phi_c))] \quad (106)$$

and

$$V^{(n)}(\phi_c) \equiv \xi(t(\phi_c))^n \frac{\partial^n}{\partial \phi(t)^n} V(\mu(t), \lambda_i(t), \phi(t)) \Big|_{t=t(\phi_c)} \quad (107)$$

Using Eq. (104) one can easily prove that¹⁴,

$$V^{(n)}(\phi_c) = \frac{d^n V(\phi_c)}{d\phi_c^n} \quad (108)$$

Fixing the scale is a matter of convention. Fixing the scale, as we have just described, as a function of ϕ_c (*i.e.* giving different scales for different values of the field) is usually done to optimize the validity of the perturbative expansion, *i.e.* minimizing the value of radiative corrections to the effective potential around the minimum of the field. A very interesting result obtained in Ref.¹³ is: *The RGE improved effective potential exact up to (next-to-leading)^L log order^c is obtained using the L-loop effective potential and the (L+1)-loop RGE β -functions.*

^cThe convention is (next-to-leading)⁰ \equiv leading, *i.e.* $L = 0$. For $L = 1$ the potential is exact to next-to-leading log.

2 Field Theory at Finite Temperature

The formalism used in conventional quantum field theory is suitable to describe observables (*e.g.* cross-sections) measured in empty space-time, as particle interactions in an accelerator. However, in the early stages of the universe, at high temperature, the environment had a non-negligible matter and radiation density, making the hypotheses of conventional field theories impracticable. For that reason, under those circumstances, the methods of conventional field theories are no longer in use, and should be replaced by others, closer to thermodynamics, where the background state is a thermal bath. This field has been called field theory at finite temperature and it is extremely useful to study all phenomena which happened in the early universe: phase transitions, inflationary cosmology, ... Excellent articles^{15,16}, review articles^{17,18,19} and textbooks²⁰ exist which discuss different aspects of these issues. In this section we will review the main methods which will be useful for the theory of phase transitions at finite temperature.

2.1 Grand-canonical ensemble

In this section we shall give some definitions borrowed from thermodynamics and statistical mechanics. The **microcanonical ensemble** is used to describe an isolated system with fixed energy E , particle number N and volume V . The **canonical ensemble** describes a system in contact with a heat reservoir at temperature T : the energy can be exchanged between them and T , N and V are fixed. Finally, in the **grand canonical ensemble** the system can exchange energy and particles with the reservoir: T , V and the chemical potentials are fixed.

Consider now a dynamical system characterized by a hamiltonian^d H and a set of conserved (mutually commuting) charges Q_A . The equilibrium state of the system at rest in the large volume V is described by the **grand-canonical density operator**

$$\rho = \exp(-\Phi) \exp \left\{ - \sum_A \alpha_A Q_A - \beta H \right\} \quad (109)$$

where $\Phi \equiv \log Tr \exp \{ - \sum_A \alpha_A Q_A - \beta H \}$ is called the Massieu function (Legendre transform of the entropy), α_A and β are Lagrange multipliers given by $\beta = T^{-1}$, $\alpha_A = -\beta \mu_A$, T is the temperature and μ_A are the chemical potentials.

^dAll operators will be considered in the Heisenberg picture.

Using (109) one defines the **grand canonical average** of an arbitrary operator \mathcal{O} , as

$$\langle \mathcal{O} \rangle \equiv Tr(\mathcal{O}\rho) \quad (110)$$

satisfying the property $\langle \mathbf{1} \rangle = 1$.

In the following of this section we will always consider the case of zero chemical potential. It will be re-introduced when necessary.

2.2 Generating functionals

We will start considering the case of a real scalar field $\phi(x)$, carrying no charges ($\mu_A = 0$), with hamiltonian H , *i.e.*

$$\phi(x) = e^{itH} \phi(0, \vec{x}) e^{-itH} \quad (111)$$

where the time $x^0 = t$ is analytically continued to the complex plane.

We define the thermal Green function as the grand canonical average of the ordered product of the n field operators

$$G^{(C)}(x_1, \dots, x_n) \equiv \langle T_C \phi(x_1), \dots, \phi(x_n) \rangle \quad (112)$$

where the T_C ordering means that fields should be ordered along the path C in the complex t -plane. For instance the product of two fields is defined as,

$$T_C \phi(x) \phi(y) = \theta_C(x^0 - y^0) \phi(x) \phi(y) + \theta_C(y^0 - x^0) \phi(y) \phi(x) \quad (113)$$

If we parameterize C as $t = z(\tau)$, where τ is a real parameter, T_C ordering means standard ordering along τ . Therefore the step and delta functions can be given as $\theta_C(t) = \theta(\tau)$, $\delta_C(t) = (\partial z / \partial \tau)^{-1} \delta(\tau)$.

The rules of the functional formalism can be applied as usual, with the prescription $\delta j(y) / \delta j(x) = \delta_C(x^0 - y^0) \delta^{(3)}(\vec{x} - \vec{y})$, and the generating functional $Z^\beta[j]$ for the full Green functions,

$$Z^\beta[j] = \sum_{n=0}^{\infty} \frac{i^n}{n!} \int_C d^4 x_1 \dots d^4 x_n j(x_1) \dots j(x_n) G^{(C)}(x_1, \dots, x_n) \quad (114)$$

can also be written as,

$$Z^\beta[j] = \left\langle T_C \exp \left\{ i \int_C d^4 x j(x) \phi(x) \right\} \right\rangle \quad (115)$$

which is normalized to $Z^\beta[0] = \langle \mathbf{1} \rangle = 1$, as in (110), and where the integral along t is supposed to follow the path C in the complex plane.

Similarly, the generating functional for connected Green functions $W^\beta[j]$ is defined as $Z^\beta[j] \equiv \exp\{iW^\beta[j]\}$, and the generating functional for 1PI Green functions $\Gamma^\beta[\bar{\phi}]$, by the Legendre transformation,

$$\Gamma^\beta[\bar{\phi}] = W^\beta[j] - \int_C d^4x \frac{\delta W^\beta[j]}{\delta j(x)} j(x) \quad (116)$$

where the current $j(x)$ is eliminated in favor of the classical field $\bar{\phi}(x)$ as $\bar{\phi}(x) = \delta W^\beta[j]/\delta j(x)$. It follows that $\delta\Gamma^\beta[\bar{\phi}]/\delta\bar{\phi}(x) = -j(x)$, and $\bar{\phi}(x) = \langle\phi(x)\rangle$ is the grand canonical average of the field $\phi(x)$.

Symmetry violation is signaled by

$$\left. \frac{\delta\Gamma^\beta[\bar{\phi}]}{\delta\bar{\phi}} \right|_{j=0} = 0 \quad (117)$$

for a value of the field different from zero.

As in field theory at zero temperature, in a translationally invariant theory $\bar{\phi}(x) = \phi_c$ is a constant. In this case, by removing the overall factor of space-time volume arising in each term of $\Gamma^\beta[\phi_c]$, we can define the effective potential at finite temperature as,

$$\Gamma^\beta[\phi_c] = - \int d^4x V_{\text{eff}}^\beta(\phi_c) \quad (118)$$

and symmetry breaking occurs when

$$\frac{\partial V_{\text{eff}}^\beta(\phi_c)}{\partial\phi_c} = 0 \quad (119)$$

for $\phi_c \neq 0$.

2.3 Green functions

Scalar fields

Not all the contours are allowed if we require Green functions to be analytic with respect to t . Using (113) we can write the two-point Green function as,

$$G^{(C)}(x-y) = \theta_C(x^0 - y^0)G_+(x-y) + \theta_C(y^0 - x^0)G_-(x-y) \quad (120)$$

where

$$G_+(x-y) = \langle\phi(x)\phi(y)\rangle, \quad G_-(x-y) = G_+(y-x) \quad (121)$$

Now, take the complete set of states $|n\rangle$ with eigenvalues E_n : $H|n\rangle = E_n|n\rangle$. One can readily compute (121) at the point $\vec{x} = \vec{y} = 0$ as

$$G_+(x^0 - y^0) = e^{-\Phi} \sum_{m,n} |\langle m|\phi(0)|n\rangle|^2 e^{-iE_n(x^0 - y^0)} e^{iE_m(x^0 - y^0 + i\beta)} \quad (122)$$

so that the convergence of the sum implies that $-\beta \leq \text{Im}(x^0 - y^0) \leq 0$ which requires $\theta_C(x^0 - y^0) = 0$ for $\text{Im}(x^0 - y^0) > 0$. From (121) it follows that the similar property for the convergence of $G_-(x^0 - y^0)$ is that $0 \leq \text{Im}(x^0 - y^0) \leq \beta$, which requires $\theta_C(y^0 - x^0) = 0$ for $\text{Im}(x^0 - y^0) < 0$, and the final condition for the convergence of the complete Green function on the strip

$$-\beta \leq \text{Im}(x^0 - y^0) \leq \beta \quad (123)$$

is that we define the function $\theta_C(t)$ such that $\theta_C(t) = 0$ for $\text{Im}(t) > 0$. The latter condition implies that C must be such that *a point moving along it has a monotonically decreasing or constant imaginary part*.

A very important periodicity relation affecting Green functions can be easily deduced from the very definition of $G_+(x)$ and $G_-(x)$, Eq. (121). By using the definition of the grand canonical average and the cyclic permutation property of the trace of a product of operators, it can be easily deduced,

$$G_+(t - i\beta, \vec{x}) = G_-(t, \vec{x}) \quad (124)$$

which is known as the Kubo-Martin-Schwinger relation²¹.

We can now compute the two-point Green function (120) for a free scalar field,

$$\phi(x) = \int \frac{d^3p}{(2\pi)^{3/2}(2\omega_p)^{1/2}} [a(p)e^{-ipx} + a^\dagger(p)e^{ipx}] \quad (125)$$

where $\omega_p = \sqrt{\vec{p}^2 + m^2}$, which satisfies the equation

$$[\partial^\mu \partial_\mu + m^2] G^{(C)}(x - y) = -i\delta_C(x - y) \equiv -i\delta_C(x^0 - y^0)\delta^{(3)}(\vec{x} - \vec{y}) \quad (126)$$

Using the time derivative of (125), and the equal time commutation relation,

$$[\phi(t, \vec{x}), \dot{\phi}(t, \vec{y})] = i\delta^{(3)}(\vec{x} - \vec{y}) \quad (127)$$

one easily obtains the commutation relation for creation and annihilation operators,

$$[a(p), a^\dagger(k)] = \delta^{(3)}(\vec{p} - \vec{k}) \quad (128)$$

and defining the Hamiltonian of the field as,

$$H = \int \frac{d^3p}{(2\pi)^3} \omega_p a^\dagger(p) a(p) \quad (129)$$

one can obtain, using (128) the thermodynamical averages,

$$\begin{aligned} \langle a^\dagger(p) a(k) \rangle &= n_B(\omega_p) \delta^{(3)}(\vec{p} - \vec{k}) \\ \langle a(p) a^\dagger(k) \rangle &= [1 + n_B(\omega_p)] \delta^{(3)}(\vec{p} - \vec{k}) \end{aligned} \quad (130)$$

where $n_B(\omega)$ is the Bose distribution function,

$$n_B(\omega) = \frac{1}{e^{\beta\omega} - 1} \quad (131)$$

We will give here a simplified derivation of expression (130). Consider the simpler example of a quantum mechanical state occupied by bosons of the **same** energy ω . There may be any number of bosons in that state and no interaction between the particles: we will denote that state by $|n\rangle$. The set $\{|n\rangle\}$ is complete. Creation and annihilation operators are denoted by a^\dagger and a , respectively. They act on the states $|n\rangle$ as, $a^\dagger|n\rangle = \sqrt{n+1}|n+1\rangle$ and $a|n\rangle = \sqrt{n}|n-1\rangle$, and satisfy the commutation relation, $[a, a^\dagger] = 1$. The hamiltonian and number operators are defined as $H = \omega N$ and $N = a^\dagger a$, with eigenvalues ωn and n , respectively.

It is very easy to compute now $\langle a^\dagger a \rangle$ and $\langle a a^\dagger \rangle$ as in (130) using the completeness of $\{|n\rangle\}$. In particular,

$$Tr(e^{-\beta H}) = \sum_{n=0}^{\infty} \langle n | e^{-\beta H} | n \rangle = \sum_{n=0}^{\infty} e^{-\beta\omega n} = \frac{1}{1 - e^{-\beta\omega}}$$

and

$$Tr(e^{-\beta H} a^\dagger a) = \sum_{n=0}^{\infty} n e^{-\beta\omega n} = \frac{e^{-\beta\omega}}{(1 - e^{-\beta\omega})^2}$$

from where $\langle a^\dagger a \rangle = n_B(\omega)$, and $\langle a a^\dagger \rangle = 1 + n_B(\omega)$, as we wanted to prove.

Using now (130) we can cast the two-point Green function as,

$$G^{(C)}(x-y) = \int \frac{d^4p}{(2\pi)^4} \rho(p) e^{-ip(x-y)} [\theta_C(x^0 - y^0) + n_B(p^0)] \quad (132)$$

where the function $\rho(p)$ is defined by $\rho(p) = 2\pi[\theta(p^0) - \theta(-p^0)]\delta(p^2 - m^2)$. Now the particular value of the Green function (132) depends on the chosen contour C . We will show later on two particular contours giving rise to the so-called imaginary and real time formalisms. Before coming to them we will describe how the previous formulae apply to the case of fermion fields.

Fermion fields

We will replace here (120) and (121) by,

$$S_{\alpha\beta}^{(C)}(x-y) \equiv \langle T_C \psi_\alpha(x) \bar{\psi}_\beta(y) \rangle = \theta_C(x^0 - y^0) S_{\alpha\beta}^+ - \theta_C(y^0 - x^0) S_{\alpha\beta}^- \quad (133)$$

where α and β are spinor indices, and

$$S_{\alpha\beta}^+(x-y) = \langle \psi_\alpha(x) \bar{\psi}_\beta(y) \rangle \quad (134)$$

are the reduced Green function, which satisfy the Kubo-Martin-Schwinger relation,

$$S_{\alpha\beta}^+(t - i\beta, \vec{x}) = -S_{\alpha\beta}^-(t, \vec{x}) \quad (135)$$

The calculation of the two-Green function for a free fermion field, satisfying the equation

$$(i\gamma \cdot \partial - m)_{\alpha\sigma} S_{\sigma\beta}^{(C)}(x-y) = i\delta_C(x-y)\delta_{\alpha\beta} \quad (136)$$

follows lines similar to Eqs. (125) to (132). In particular, one can define a Green function $S^{(C)}$ as

$$S_{\alpha\beta}^{(C)}(x-y) \equiv (i\gamma \cdot \partial + m)_{\alpha\beta} S^{(C)}(x-y) \quad (137)$$

where $S^{(C)}(x-y)$ satisfies the Klein-Gordon propagator equation (126). One can obtain for $S^{(C)}$ the expression,

$$S^{(C)}(x-y) = \int \frac{d^4p}{(2\pi)^4} \rho(p) e^{-ip(x-y)} [\theta_C(x^0 - y^0) - n_F(p^0)] \quad (138)$$

where $n_F(\omega)$ is the Fermi distribution function

$$n_F(\omega) = \frac{1}{e^{\beta\omega} + 1}. \quad (139)$$

Eq. (139) can be derived similarly to (131) as the mean number of fermions for a Fermi gas. This time the Pauli exclusion principle forbids more than one fermion occupying a single state, so that only the states $|0\rangle$ and $|1\rangle$ exist. They are acted on by creation and annihilation operators b^\dagger and b , respectively as: $b^\dagger|0\rangle = |1\rangle$, $b^\dagger|1\rangle = 0$, $b|0\rangle = 0$, $b|1\rangle = |0\rangle$, and satisfy anticommutation rules, $\{b, b^\dagger\} = 1$. Defining the hamiltonian and number operators as $H = \omega N$ and $N = b^\dagger b$, we can compute now the statistical averages of $\langle b^\dagger b \rangle$ and $\langle bb^\dagger \rangle$ using the completeness of $\{|n\rangle\}$.

$$Tr(e^{-\beta H}) = \sum_{n=0}^1 \langle n | e^{-\beta H} | n \rangle = \sum_{n=0}^1 e^{-\beta\omega n} = 1 + e^{-\beta\omega}$$

and

$$\text{Tr}(e^{-\beta H} b^\dagger b) = \sum_{n=0}^1 n e^{-\beta \omega n} = e^{-\beta \omega}$$

from where $\langle b^\dagger b \rangle = n_F(\omega)$, and $\langle b b^\dagger \rangle = 1 - n_F(\omega)$, as we wanted to prove.

2.4 Imaginary time formalism

The calculation of the propagators in the previous sections depends on the chosen path C going from an initial arbitrary time t to $t - i\beta$, provided by the Kubo-Martin-Schwinger periodicity properties (124) and (135) of Green functions. The simplest path is to take a straight line along the imaginary axis $t = -i\tau$. It is called Matsubara contour, since Matsubara²² was the first to set up a perturbation theory based upon this contour. In that case $\delta_C(t) = i\delta(\tau)$.

The two-point Green functions for scalar (132) and fermion (138) fields can be written as,

$$G(\tau, \vec{x}) = \int \frac{d^4 p}{(2\pi)^4} \rho(p) e^{i\vec{p}\vec{x}} e^{-\tau p^0} [\theta(\tau) + \eta n(p^0)] \quad (140)$$

where the symbol η stands as: $\eta_B = 1$ ($\eta_F = -1$) for bosons (for fermions). Analogously, $n(p^0)$ stands either for $n_B(p^0)$, as given by (131) for bosons, or $n_F(p^0)$, as given by (139) for fermions. It can be defined as a function of η as,

$$n(\omega) = \frac{1}{e^{\beta\omega} - \eta} \quad (141)$$

The Green function (140) can be decomposed as in (120)

$$G(\tau, \vec{x}) = G_+(\tau, \vec{x})\theta(\tau) + G_-(\tau, \vec{x})\theta(-\tau) \quad (142)$$

Using now the Kubo-Martin-Schwinger relations, Eqs. (124) and (135), we can write $G(\tau + \beta) = \eta G(\tau)$ for $-\beta \leq \tau \leq 0$, $G(\tau - \beta) = \eta G(\tau)$ for $0 \leq \tau \leq \beta$, which means that the propagator for bosons (fermions) is periodic (antiperiodic) in the *time* variable τ , with period β .

It follows that the Fourier transform of (140)

$$\tilde{G}(\omega_n, \vec{p}) = \int_{\alpha-\beta}^{\alpha} d\tau \int d^3 x e^{i\omega_n \tau - i\vec{x}\vec{p}} G(\tau, \vec{x}) \quad (143)$$

(where $0 \leq \alpha \leq \beta$) is independent of α and the discrete frequencies satisfy the relation $\eta e^{i\omega_n \beta} = 1$, *i.e.* $\omega_n = 2n\pi\beta^{-1}$ for bosons, and $\omega_n = (2n + 1)\pi\beta^{-1}$ for fermions.

Inserting now (140) into (143) we can obtain the propagator in momentum space \tilde{G}

$$\tilde{G}(\omega_n, \vec{p}) = \frac{1}{\vec{p}^2 + m^2 + \omega_n^2}. \quad (144)$$

We can now define the euclidean propagator, $\Delta(-i\tau, \vec{x})$, by

$$G(\tau, \vec{x}) = i\Delta(-i\tau, \vec{x}) \quad (145)$$

where $G(\tau, \vec{x})$ is the propagator defined in (140). Therefore, using (144), we can write the inverse Fourier transformation,

$$\Delta(x) = \frac{1}{\beta} \sum_{n=-\infty}^{\infty} \int \frac{d^3p}{(2\pi)^3} e^{-i\omega_n\tau + i\vec{p}\vec{x}} \frac{-i}{\vec{p}^2 + m^2 + \omega_n^2} \quad (146)$$

where the Matsubara frequencies ω_n are either for bosons or for fermions.

From (146) one can deduce the Feynman rules for the different fields in the imaginary time formalism. We can summarize them in the following way:

$$\begin{aligned} \text{Boson propagator} & : \frac{i}{p^2 - m^2}; p^\mu = [2n\pi\beta^{-1}, \vec{p}] \\ \text{Fermion propagator} & : \frac{i}{\gamma \cdot p - m}; p^\mu = [(2n+1)\pi\beta^{-1}, \vec{p}] \\ \text{Loop integral} & : \frac{i}{\beta} \sum_{n=-\infty}^{\infty} \int \frac{d^3p}{(2\pi)^3} \\ \text{Vertex function} & : -i\beta(2\pi)^3 \delta_{\sum \omega_i} \delta^{(3)}(\sum_i \vec{p}_i) \end{aligned} \quad (147)$$

There is a standard trick to perform infinite summations as in (147). For the case of bosons we can have frequency sums as,

$$\frac{1}{\beta} \sum_{n=-\infty}^{\infty} f(p^0 = i\omega_n) \quad (148)$$

with $\omega_n = 2n\pi\beta^{-1}$. Since the function $\frac{1}{2}\beta \coth(\frac{1}{2}\beta z)$ has poles at $z = i\omega_n$ and is analytic and bounded everywhere else, we can write (148) as,

$$\frac{1}{2\pi i\beta} \int_{\gamma} dz f(z) \frac{\beta}{2} \coth(\frac{1}{2}\beta z)$$

where the contour γ encircles anticlockwise all the previous poles of the imaginary axis. We are assuming that $f(z)$ does not have singularities along the imaginary axis (otherwise the previous expression is obviously not correct). The contour γ can be deformed to a new contour consisting in two straight lines: the first one starting at $-i\infty + \epsilon$ and going to $i\infty + \epsilon$, and the second one starting at $i\infty - \epsilon$ and ending at $-i\infty - \epsilon$. Rearranging the exponentials in the hyperbolic cotangent one can write the previous expression as,

$$\frac{1}{2\pi i} \int_{-i\infty}^{i\infty} dz \frac{1}{2} [f(z) + f(-z)] + \frac{1}{2\pi i} \int_{-i\infty+\epsilon}^{i\infty+\epsilon} dz [f(z) + f(-z)] \frac{1}{e^{\beta z} - 1}$$

and the contour of the second integral can be deformed to a contour C which encircles clockwise all singularities of the functions $f(z)$ and $f(-z)$ in the right half plane. Therefore we can write (148) as

$$\frac{1}{\beta} \sum_{n=-\infty}^{\infty} f(p^0 = i\omega_n) = \int_{-i\infty}^{i\infty} \frac{dz}{4\pi i} [f(z) + f(-z)] + \int_C \frac{dz}{2\pi i} n_B(z) [f(z) + f(-z)] \quad (149)$$

where $n_B(z)$ is the Bose distribution function (131).

Eq. (149) can be generalized for both bosons and fermions as,

$$\frac{1}{\beta} \sum_{n=-\infty}^{\infty} f(p^0 = i\omega_n) = \int_{-i\infty}^{i\infty} \frac{dz}{4\pi i} [f(z) + f(-z)] + \eta \int_C \frac{dz}{2\pi i} n(z) [f(z) + f(-z)] \quad (150)$$

where the distribution functions $n(z)$ are defined in (141). Eq. (150) shows that the frequency sum naturally separates into a T independent piece, which should coincide with the similar quantity computed in the field theory at zero temperature, and a T dependent piece which vanishes in the limit $T \rightarrow 0$, *i.e.* $\beta \rightarrow \infty$.

2.5 Real time formalism

The obvious disadvantage of the imaginary time formalism is to compute Green functions along imaginary time, so that going to the real time has to be done through a process of analytic continuation. However, a direct evaluation of Green function in the real time is possible by a judicious choice of the contour C in (112). The family of such real time contours is depicted in Fig. 4 where the contour C is $C = C_1 \cup C_2 \cup C_3 \cup C_4$ where C_1 goes from the initial time t_i to the final time t_f , C_3 from t_f to $t_f - i\sigma$, with $0 \leq \sigma \leq \beta$, C_2 from $t_f - i\sigma$ to $t_i - i\sigma$, and C_4 from $t_i - i\sigma$ to $t_i - i\beta$. Different choices of σ lead

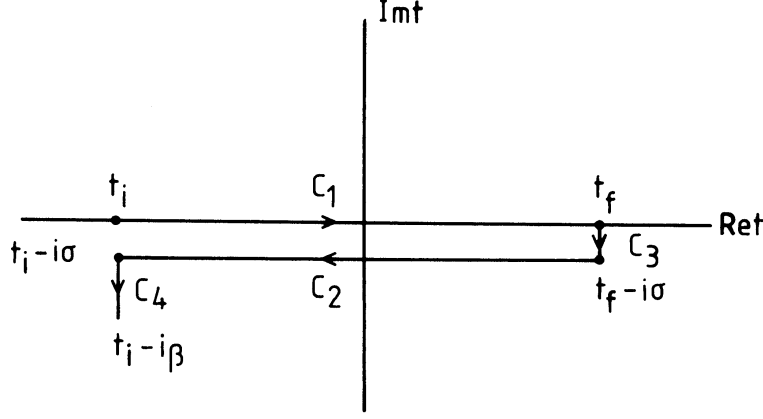


Figure 4: Contour used in the real time formalism.

to an equivalence class of quantum field theories at finite temperature²³. For instance the choice $\sigma = 0$ leads to the Keldysh perturbation expansion²⁴, while the choice $\sigma = \beta/2$ is the preferred one to compute Green functions.

Computing the Green function for scalar (132) and fermion (138) fields taking path C is a matter of calculation, as we did for the imaginary time formalism in (140)-(144). One can prove that the contribution from the contours C_3 and C_4 can be neglected^{18,25}. Therefore, for the propagator between x^0 and y^0 there are four possibilities depending on whether they are on C_1 or C_2 . Correspondingly, there are four propagators which are labeled by (11), (12), (21) and (22).

Making the choice $\sigma = \beta/2$, the propagators for scalar fields (132) can be written, in momentum space, as

$$G(p) \equiv \begin{pmatrix} G^{(11)}(p) & G^{(12)}(p) \\ G^{(21)}(p) & G^{(22)}(p) \end{pmatrix} = M_B(\beta, p) \begin{pmatrix} \Delta(p) & 0 \\ 0 & \Delta^*(p) \end{pmatrix} M_B(\beta, p) \quad (151)$$

where $\Delta(p)$ is the boson propagator at zero temperature, and the matrix $M_B(\beta, p)$ is given by,

$$M_B(\beta, p) = \begin{pmatrix} \cosh \theta(p) & \sinh \theta(p) \\ \sinh \theta(p) & \cosh \theta(p) \end{pmatrix} \quad (152)$$

where

$$\sinh \theta(p) = e^{-\beta\omega_p/2} (1 - e^{-\beta\omega_p})^{-1/2}$$

$$\cosh \theta(p) = (1 - e^{-\beta\omega_p})^{-1/2} \quad (153)$$

Using now (151), (152), (153), one can easily write the expression for the four bosonic propagators, as

$$\begin{aligned} G^{(11)}(p) &= \Delta(p) + 2\pi n_B(\omega_p)\delta(p^2 - m^2) \\ G^{(22)}(p) &= G^{(11)*} \\ G^{(12)} &= 2\pi e^{\beta\omega_p/2} n_B(\omega_p)\delta(p^2 - m^2) \\ G^{(21)} &= G^{(12)} \end{aligned} \quad (154)$$

Similarly, the propagators for fermion fields can be written as

$$\begin{aligned} S(p)_{\alpha\beta} &\equiv \begin{pmatrix} S_{\alpha\beta}^{(11)}(p) & S_{\alpha\beta}^{(12)}(p) \\ S_{\alpha\beta}^{(21)}(p) & S_{\alpha\beta}^{(22)}(p) \end{pmatrix} \\ &= M_F(\beta, p) \begin{pmatrix} (\gamma \cdot p + m)_{\alpha\beta} \Delta(p) & 0 \\ 0 & (\gamma \cdot p + m)_{\alpha\beta} \Delta^*(p) \end{pmatrix} M_F(\beta, p) \end{aligned} \quad (155)$$

where the matrix $M_F(\beta, p)$ is,

$$M_F(\beta, p) = \begin{pmatrix} \cos \theta(p) & \sin \theta(p) \\ \sin \theta(p) & \cos \theta(p) \end{pmatrix} \quad (156)$$

with

$$\begin{aligned} \sin \theta(p) &= e^{-\beta\omega_p/2} (1 + e^{-\beta\omega_p})^{-1/2} \\ \cos \theta(p) &= [\theta(p^0) - \theta(-p^0)] (1 + e^{-\beta\omega_p})^{-1/2} \end{aligned} \quad (157)$$

In the same way, using now (155), (156), and (157) one can easily write the expression for the four fermionic propagators, as

$$\begin{aligned} S^{(11)}(p) &= (\gamma \cdot p + m) (\Delta(p) - 2\pi n_F(\omega_p)\delta(p^2 - m^2)) \\ S^{(22)}(p) &= S^{(11)*} \\ S^{(12)} &= -2\pi(\gamma \cdot p + m)[\theta(p^0) - \theta(-p^0)]e^{\beta\omega_p/2} n_F(\omega_p)\delta(p^2 - m^2) \\ S^{(21)} &= -S^{(12)} \end{aligned} \quad (158)$$

As one can see from (154) and (158), the main feature of the real time formalism is that the propagators come in two terms: one which is the same as in the zero temperature field theory, and a second one where all the temperature dependence is contained. This is welcome. However the propagators

(12), (21) and (22) are unphysical since one of their time arguments has an imaginary component. They are required for the consistency of the theory. The only physical propagator is the (11) component in (154) and (158).

Now the Feynman rules in the real time formalism are very similar to those in the zero temperature field theory. In fact all diagrams have the same topology as in the zero temperature field theory and the same symmetry factors. However, associated to every field there are two possible vertices, 1 and 2, and four possible propagators, (11), (12), (21) and (22) connecting them. All of them have to be considered for the consistency of the theory. In the Feynman rules, type 2 vertices are hermitian conjugate with respect to type 1 vertices. The golden rule is that: *physical legs must always be attached to type 1 vertices*. Apart from the previous prescription, one must sum over all the configurations of type 1 and type 2 vertices, and use the propagator $G^{(ab)}$ or $S^{(ab)}$ to connect vertex a with vertex b .

There is now a general agreement in the sense that the imaginary time formalism and the real time formalism should give the same physical answer²⁶. Using one or the other is sometimes a matter of taste, though in some cases the choice is dictated by calculational simplicity depending on the physical problem one is dealing with.

3 The effective potential at finite temperature

In this section we will construct the (one-loop) effective potential at finite temperature, using all the tools provided in the previous sections. As we will see, in particular, the effective potential at finite temperature contains the effective potential at zero temperature computed in section 1. The usefulness of this construction is addressed to the theory of phase transitions at finite temperature. The latter being essential for the understanding of phenomena as: inflation, baryon asymmetry generation, quark-gluon plasma transition in QCD,... We will compare different methods leading to the same result, including the use of both the imaginary and the real time formalisms. This exercise can be useful mainly to face more complicated problems than those which will be developed in this course.

3.1 Scalar fields

We will consider here the simplest model of one self-interacting scalar fields described by the lagrangian (22) and (23). We have to compute the diagrams contained in Fig. 1 using the Feynman rules described in (147), for the imaginary time formalism, or in (154) for the real time formalism. We will write

the result as,

$$V_{\text{eff}}^\beta(\phi_c) = V_0(\phi_c) + V_1^\beta(\phi_c) \quad (159)$$

where $V_0(\phi_c)$ is the tree level potential.

Imaginary time formalism

We will compute the diagrams in Fig. 1. Using the Feynman rules in Eq. (147), Eq. (28) translates into,

$$V_1^\beta(\phi_c) = \frac{1}{2\beta} \sum_{n=-\infty}^{\infty} \int \frac{d^3p}{(2\pi)^3} \log(\omega_n^2 + \omega^2) \quad (160)$$

where ω_n are the bosonic Matsubara frequencies and

$$\omega^2 = \vec{p}^2 + m^2(\phi_c) \quad (161)$$

m^2 being defined in (27).

The sum over n in (160) diverges, but the infinite part does not depend on ϕ_c . The finite part, which contains the ϕ_c dependence, can be computed by the following method¹⁵. Define,

$$v(\omega) = \sum_{n=-\infty}^{\infty} \log(\omega_n^2 + \omega^2) \quad (162)$$

then,

$$\frac{\partial v}{\partial \omega} = \sum_{n=-\infty}^{\infty} \frac{2\omega}{\omega_n^2 + \omega^2} \quad (163)$$

Using the identity,

$$\begin{aligned} f(y) = \sum_{n=1}^{\infty} \frac{y}{y^2 + n^2} &= -\frac{1}{2y} + \frac{1}{2}\pi \coth \pi y \\ &= -\frac{1}{2y} + \frac{\pi}{2} + \pi \frac{e^{-2\pi y}}{1 - e^{-2\pi y}} \end{aligned} \quad (164)$$

with $y = \beta\omega/2\pi$ we obtain,

$$\frac{\partial v}{\partial \omega} = 2\beta \left[\frac{1}{2} + \frac{e^{-\beta\omega}}{1 - e^{-\beta\omega}} \right] \quad (165)$$

and

$$v(\omega) = 2\beta \left[\frac{\omega}{2} + \frac{1}{\beta} \log(1 - e^{-\beta\omega}) \right] + \omega - \text{independent terms} \quad (166)$$

Substituting finally (166) into (160) one gets,

$$V_1^\beta(\phi_c) = \int \frac{d^3p}{(2\pi)^3} \left[\frac{\omega}{2} + \frac{1}{\beta} \log(1 - e^{-\beta\omega}) \right] \quad (167)$$

One can easily prove that the first integral in (167) is the one-loop effective potential at zero temperature. For that we have to prove the identity,

$$-\frac{i}{2} \int_{-\infty}^{\infty} \frac{dx}{2\pi} \log(-x^2 + \omega^2 - i\epsilon) = \frac{\omega}{2} + \text{constant} \quad (168)$$

i.e.

$$\omega \int_{-\infty}^{\infty} \frac{dx}{2\pi i} \frac{1}{-x^2 + \omega^2 - i\epsilon} = \frac{1}{2} \quad (169)$$

Integral (169) can be performed closing the integration interval $(-\infty, \infty)$ in the complex x plane along a contour going anticlockwise and picking the pole of the integrand at $x = -\sqrt{\omega^2 - i\epsilon}$ with a residue $1/2\omega$. Using the residues theorem Eq. (169) can be easily checked. Now we can use identity (168) to write the temperature independent part of (167) as

$$\frac{1}{2} \int \frac{d^3p}{(2\pi)^3} \omega = -\frac{i}{2} \int \frac{d^4p}{(2\pi)^4} \log(-p_0^2 + \omega^2 - i\epsilon) \quad (170)$$

and, after making the Wick rotation $p^0 = ip_E$ in (170) we obtain,

$$\frac{1}{2} \int \frac{d^3p}{(2\pi)^3} \omega = \frac{1}{2} \int \frac{d^4p}{(2\pi)^4} \log[p^2 + m^2(\phi_c)] \quad (171)$$

which is the same result we obtained in the zero temperature field theory, see Eq. (28).

Now the temperature dependent part in (167) can be easily written as,

$$\frac{1}{\beta} \int \frac{d^3p}{(2\pi)^3} \log(1 - e^{-\beta\omega}) = \frac{1}{2\pi^2\beta^4} J_B[m^2(\phi_c)\beta^2] \quad (172)$$

where the thermal bosonic function J_B is defined as,

$$J_B[m^2\beta^2] = \int_0^\infty dx x^2 \log \left[1 - e^{-\sqrt{x^2 + \beta^2 m^2}} \right] \quad (173)$$

The integral (173) and therefore the thermal bosonic effective potential admits a high-temperature expansion which will be very useful for practical applications. It is given by

$$J_B(m^2/T^2) = -\frac{\pi^4}{45} + \frac{\pi^2 m^2}{12 T^2} - \frac{\pi}{6} \left(\frac{m^2}{T^2}\right)^{3/2} - \frac{1}{32} \frac{m^4}{T^4} \log \frac{m^2}{a_b T^2} \quad (174)$$

$$- 2\pi^{7/2} \sum_{\ell=1}^{\infty} (-1)^\ell \frac{\zeta(2\ell+1)}{(\ell+1)!} \Gamma\left(\ell + \frac{1}{2}\right) \left(\frac{m^2}{4\pi^2 T^2}\right)^{\ell+2}$$

where $a_b = 16\pi^2 \exp(3/2 - 2\gamma_E)$ ($\log a_b = 5.4076$) and ζ is the Riemann ζ -function.

There is a very simple way of computing the effective potential: it consists in *computing its derivative in the shifted theory and then integrating!* In fact the derivative of the effective potential

$$\frac{dV_1^\beta}{d\phi_c}$$

is described diagrammatically by the tadpole diagram. In fact using the Feynman rules in (147) one can easily write for the tadpole the expression,

$$\frac{dV_1^\beta}{d\phi_c} = \frac{\lambda\phi_c}{2} \frac{1}{\beta} \sum_{n=-\infty}^{\infty} \int \frac{d^3p}{(2\pi)^3} \frac{1}{\omega_n^2 + \omega^2} \quad (175)$$

or, using the expression (27) for $m^2(\phi_c)$,

$$\frac{dV_1^\beta}{dm^2(\phi_c)} = \frac{1}{2\beta} \sum_{n=-\infty}^{\infty} \int \frac{d^3p}{(2\pi)^3} \frac{1}{\omega_n^2 + \omega^2} \quad (176)$$

Now we can perform the infinite sum in (176) using the result in Eq. (149) with a function f defined as,

$$f(z) = \frac{1}{\omega^2 - z^2} \quad (177)$$

and obtain for the tadpole (176) the result

$$\frac{dV_1^\beta}{dm^2(\phi_c)} = \int \frac{d^3p}{(2\pi)^3} \left\{ \frac{1}{2} \int_{-i\infty}^{i\infty} \frac{dz}{2\pi i} \frac{1}{\omega^2 - z^2} + \int_C \frac{dz}{2\pi i} \frac{1}{e^{\beta z} - 1} \frac{1}{\omega^2 - z^2} \right\} \quad (178)$$

The first term in (178) gives the β -independent part of the tadpole contribution as,

$$\frac{1}{2} \int_{-i\infty}^{i\infty} \frac{dz}{2\pi i} \frac{1}{\omega^2 - z^2} \quad (179)$$

We can now close the integration contour of (179) anticlockwise and pick the pole of (177) at $z = -\omega$ with a residue $1/2\omega$. The result of (179) is

$$\frac{1}{4\omega} \quad (180)$$

The second term in (178) gives the β -dependent part of the tadpole contribution. Here the integration contour encircles the pole at $z = \omega$ with a residue

$$-\frac{1}{2\omega} \frac{1}{e^{\beta\omega} - 1} \quad (181)$$

Adding (180) and (181) we obtain for the tadpole the final expression,

$$\frac{dV_1(\phi_c)}{dm^2(\phi_c)} = \frac{1}{2} \int \frac{d^3p}{(2\pi)^3} \left[\frac{1}{2\omega} + \frac{1}{\omega} \frac{1}{e^{\beta\omega} - 1} \right] \quad (182)$$

Now, integration of (182) with respect to $m^2(\phi_c)$ leads to the expression (167) for the thermal effective potential and, therefore, to the final expression given by (171) and (172).

Real time formalism

As we will see in this section, the final result for the effective potential (167) can be also obtained using the real time formalism. Let us compute the tadpole diagram. Since physical legs must be attached to type 1 vertices, the vertex in the tadpole must be considered of type 1, and the propagator circulating around the loop has to be considered as a (11) propagator. Application of the Feynman rules (154) to the tadpole diagram leads to the expression ^e

$$\frac{dV_1^\beta}{d\phi_c} = \frac{\lambda\phi_c}{2} \int \frac{d^4p}{(2\pi)^4} \left[\frac{i}{p^2 - m^2(\phi_c) + i\epsilon} + 2\pi n_B(\omega)\delta(p^2 - m^2(\phi_c)) \right] \quad (183)$$

or, using as before the expression (27) for $m^2(\phi_c)$,

$$\frac{dV_1^\beta}{dm^2(\phi_c)} = \frac{1}{2} \int \frac{d^4p}{(2\pi)^4} \left[\frac{-i}{-p^2 + m^2(\phi_c) - i\epsilon} + 2\pi n_B(\omega)\delta(p^2 - m^2(\phi_c)) \right] \quad (184)$$

^eWe are replacing in (154) the value of ω_p by the corresponding value ω given by (161) in the shifted theory.

Now the β -independent part of (184), after integration on $m^2(\phi_c)$ contributes to the effective potential as

$$-\frac{i}{2} \int \frac{d^4 p}{(2\pi)^4} \log(-p^2 + m^2(\phi_c) - i\epsilon) \quad (185)$$

Finally using Eq. (168) to perform the p^0 integral, we can cast Eq. (185) as

$$\int \frac{d^3 p}{(2\pi)^3} \frac{\omega}{2} \quad (186)$$

which coincides with the first term in (167).

Integration over p^0 in the β -dependent part of (184) can be easily performed with the help of the identity

$$\delta(p^2 - m^2) = \frac{1}{2\omega_p} [\delta(p^0 + \omega_p) + \delta(p^0 - \omega_p)] \quad (187)$$

leading to,

$$\int \frac{d^3 p}{(2\pi)^3} \frac{1}{2\omega} n_B(\omega) \quad (188)$$

which, upon integration over $m^2(\phi_c)$ leads to the second term of Eq. (167).

We have checked that trivially the real time and imaginary time formalisms lead to the same expression of the thermal effective potential, in the one loop approximation.

3.2 Fermion fields

We will consider here a theory with fermion fields described by the lagrangian (32). As in the scalar case, we have to compute the diagrams contained in Fig. 2, using the Feynman rules either for the imaginary or for the real time formalism, and decompose the thermal effective potential as in (159).

Imaginary time formalism

The calculation of the diagrams in Fig. 2, using the Feynman rules (147), yields,

$$V_1^\beta(\phi_c) = -\frac{2\lambda}{2\beta} \sum_{n=-\infty}^{\infty} \int \frac{d^3 p}{(2\pi)^3} \log(\omega_n^2 + \omega^2) \quad (189)$$

where ω_n are the fermionic Matsubara frequencies and

$$\omega^2 = \vec{p}^2 + M_f^2. \quad (190)$$

The sum over n is done with the help of the same trick employed in (162)-(166). Let $f(y)$ be given by (164), then,

$$\begin{aligned}\sum_{m=2,4,\dots} \frac{y}{y^2 + m^2} &= \sum_{n=1}^{\infty} \frac{y}{y^2 + 4n^2} = \frac{1}{2} f\left(\frac{y}{2}\right) \\ \sum_{m=1,3,\dots} \frac{y}{y^2 + m^2} &= f(y) - \frac{1}{2} f\left(\frac{y}{2}\right)\end{aligned}\quad (191)$$

and using (164) we get,

$$\sum_{m=1,3,\dots} \frac{y}{y^2 + m^2} = \frac{\pi}{4} - \frac{\pi}{2} \frac{1}{e^{\pi y} + 1} \quad (192)$$

The function $v(\omega)$ in this case can be written as,

$$v(\omega) = 2 \sum_{n=1,3,\dots} \log \left[\frac{\pi^2 n^2}{\beta^2} + \omega^2 \right] \quad (193)$$

and its derivative,

$$\frac{\partial v}{\partial \omega} = \frac{4\beta}{\pi} \sum_{1,3,\dots} \frac{y}{y^2 + n^2} \quad (194)$$

where $y = \beta\omega/\pi$. Then using (192) we get

$$\frac{\partial v}{\partial \omega} = 2\beta \left[\frac{1}{2} - \frac{1}{1 + e^{\beta\omega}} \right] \quad (195)$$

and, after integration with respect to ω ,

$$v(\omega) = 2\beta \left[\frac{\omega}{2} + \frac{1}{\beta} \log(1 + e^{-\beta\omega}) \right] + \omega - \text{independent terms} \quad (196)$$

Replacing finally (196) into (189) one gets,

$$V_1^\beta(\phi_c) = -2\lambda \int \frac{d^3 p}{(2\pi)^3} \left[\frac{\omega}{2} + \frac{1}{\beta} \log(1 + e^{-\beta\omega}) \right] \quad (197)$$

The first integral in (197) can be proven, as in (168)-(171), to lead to the one-loop effective potential at zero temperature (35). The second integral, which contains all the temperature dependent part, can be written as,

$$-2\lambda \frac{1}{\beta} \int \frac{d^3 p}{(2\pi)^3} \log(1 + e^{-\beta\omega}) = -2\lambda \frac{1}{2\pi^2 \beta^4} J_F[M_f^2(\phi_c)\beta^2] \quad (198)$$

where the thermal fermionic function J_F is defined as,

$$J_F[m^2\beta^2] = \int_0^\infty dx x^2 \log \left[1 + e^{-\sqrt{x^2 + \beta^2 m^2}} \right] \quad (199)$$

As in the scalar field, the integral (199) and therefore the thermal fermionic effective potential admits a high-temperature expansion which will be very useful for practical applications. It is given by

$$\begin{aligned} J_F(m^2/T^2) &= \frac{7\pi^4}{360} - \frac{\pi^2 m^2}{24 T^2} - \frac{1}{32} \frac{m^4}{T^4} \log \frac{m^2}{a_f T^2} \\ &\quad - \frac{\pi^{7/2}}{4} \sum_{\ell=1}^{\infty} (-1)^\ell \frac{\zeta(2\ell+1)}{(\ell+1)!} (1 - 2^{-2\ell-1}) \Gamma\left(\ell + \frac{1}{2}\right) \left(\frac{m^2}{\pi^2 T^2}\right)^{\ell+2} \end{aligned} \quad (200)$$

where $a_f = \pi^2 \exp(3/2 - 2\gamma_E)$ ($\log a_f = 2.6351$) and ζ is the Riemann ζ -function.

As we did in the case of the scalar field, there is a very simple way of obtaining the effective potential, computing the tadpole in the shifted theory, and integrating over ϕ_c . Using for the fermion propagator (147)

$$i \frac{\gamma \cdot p + M_f}{p^2 - M_f^2}$$

and the trace formula,

$$Tr(\gamma \cdot p + M_f) = 2\lambda M_f$$

we can write for the tadpole the expression,

$$\frac{dV_1^\beta}{d\phi_c} = -2\lambda \Gamma M_f \frac{1}{\beta} \sum_{n=-\infty}^{\infty} \int \frac{d^3 p}{(2\pi)^3} \frac{1}{\omega_n^2 + \omega^2} \quad (201)$$

or, using the expression $M_f(\phi_c) = \Gamma \phi_c$, where Γ is the Yukawa coupling,

$$\frac{dV_1^\beta}{dM_f^2(\phi_c)} = -2\lambda \frac{1}{2\beta} \sum_{n=-\infty}^{\infty} \int \frac{d^3 p}{(2\pi)^3} \frac{1}{\omega_n^2 + \omega^2} \quad (202)$$

Now the infinite sum in (202) can be done with the help of (150), with $f(z)$ given by (177), as

$$\frac{dV_1^\beta}{dM_f^2(\phi_c)} = -2\lambda \int \frac{d^3 p}{(2\pi)^3} \left\{ \frac{1}{2} \int_{-i\infty}^{i\infty} \frac{dz}{2\pi i} \frac{1}{\omega^2 - z^2} - \int_C \frac{dz}{2\pi i} \frac{1}{e^{\beta z} + 1} \frac{1}{\omega^2 - z^2} \right\} \quad (203)$$

The first term of (203) reproduces the zero temperature result (35), after M_f^2 integration, by closing the integration contour of (179) anticlockwise and picking the pole at $z = -\omega$ with a residue $1/2\omega$. The second term in (203) gives the β -dependent part of the tadpole contribution. Here the integration contour C encircles the pole at $z = \omega$ with a residue

$$(-2\lambda)\frac{1}{2\omega}\frac{1}{e^{\beta\omega} + 1} \quad (204)$$

Adding all of them together, we obtain for the tadpole the final expression

$$\frac{dV_1(\phi_c)}{dM_f^2(\phi_c)} = -\lambda \int \frac{d^3p}{(2\pi)^3} \left[\frac{1}{2\omega} - \frac{1}{\omega} \frac{1}{e^{\beta\omega} + 1} \right] \quad (205)$$

and, upon integration with respect to M_f^2 we obtain the result previously presented in Eq. (197).

Real time formalism

As for the case of scalar fields, the thermal effective potential for fermions (197) can also be very easily obtained using the real time formalism. We compute again the tadpole diagram, where the vertex between the two fermions and the scalar is of type 1 and the fermion propagator circulating along the loop is a (11) propagator. Application of the Feynman rules (158) leads to the expression

$$\frac{dV_1^\beta}{d\phi_c} = -\Gamma Tr \int \frac{d^4p}{(2\pi)^4} (\gamma \cdot p + M_f) \left[\frac{i}{p^2 - M_f^2 + i\epsilon} - 2\pi n_F(\omega) \delta(p^2 - M_f^2) \right] \quad (206)$$

or, using as before the expression for M_f^2 ,

$$\frac{dV_1^\beta}{dM_f^2(\phi_c)} = -\frac{Tr \mathbf{1}}{2} \int \frac{d^4p}{(2\pi)^4} \left[\frac{-i}{-p^2 + M_f^2 - i\epsilon} - 2\pi n_F(\omega) \delta(p^2 - M_f^2) \right] \quad (207)$$

Now the β -independent part of (207), after integration on M_f^2 , contributes to the effective potential,

$$- Tr \mathbf{1} \int \frac{d^3p}{(2\pi)^3} \frac{\omega}{2} \quad (208)$$

which coincides with the first term in (197).

Integration over p^0 in the β -dependent part of (207) can be easily performed with the help of the identity (187) leading to,

$$- Tr \mathbf{1} \int \frac{d^3 p}{(2\pi)^3} \frac{1}{2\omega} [-n_F(\omega)] \quad (209)$$

which, upon integration over M_f^2 leads to the second term of Eq. (197).

3.3 Gauge bosons

The thermal effective potential for gauge bosons in a theory described by the lagrangian (36) is computed in the same way as for previous fields. The simplest thing is to compute the tadpole diagram using the shifted mass for the gauge boson. In the Landau gauge, the gauge boson propagator reads as,

$$\Pi_\nu^\mu(p)^{(\alpha\beta)} = \Delta_\nu^\mu G^{(\alpha\beta)}(p) \quad (210)$$

where Δ is the projector defined in (38) with a trace equal to 3 (see Eq. (41)). Therefore the final expression for the thermal effective potential is computed as,

$$V_1^\beta(\phi_c) = Tr(\Delta) \left\{ \frac{1}{2} \int \frac{d^4 p}{(2\pi)^4} \log[p^2 + M_{gb}^2(\phi_c)] + \frac{1}{2\pi^2 \beta^4} J_B[M_{gb}^2(\phi_c)\beta^2] \right\} \quad (211)$$

where the thermal bosonic function J_B in (173). The first term of (211) agrees with the zero temperature effective potential computed in (42), and the second one just counts that of a scalar field theory a number of times equal to the number of degrees of freedom (3) of the gauge boson.

3.4 The Standard Model case

The Standard Model of electroweak interactions was previously defined through Eqs. (78)-(82), and the corresponding one loop effective potential at zero temperature computed through Eqs. (83)-(91) using various renormalization schemes and the contribution of gauge and Higgs bosons and the top quark fermion to radiative corrections. Here we will compute the corresponding one loop effective potential at finite temperature. We will use the renormalization scheme of Eq. (88), so that the renormalized effective potential at zero temperature is given by Eq. (90), and consider only the contribution of W and Z bosons, and the top quark to radiative corrections. This is expected to be a good enough approximation for Higgs masses lighter than the W mass.

Using Eqs. (198) and (211) one can easily see that the finite-temperature part of the one-loop effective potential can be written as,

$$\Delta V^{(1)}(\phi_c, T) = \frac{T^4}{2\pi^2} \left[\sum_{i=W,Z} n_i J_B[m_i^2(\phi_c)/T^2] + n_t J_F[m_t^2(\phi_c)/T^2] \right] \quad (212)$$

where the function J_B and J_F where defined in Eqs. (173) and (199), respectively.

Using now the high temperature expansions (174) and (200), and the one loop effective potential at zero temperature, Eq. (90), one can write the total potential as,

$$V(\phi_c, T) = D(T^2 - T_o^2)\phi_c^2 - ET\phi_c^3 + \frac{\lambda(T)}{4}\phi_c^4 \quad (213)$$

where the coefficients are given by

$$D = \frac{2m_W^2 + m_Z^2 + 2m_t^2}{8v^2} \quad (214)$$

$$E = \frac{2m_W^3 + m_Z^3}{4\pi v^3} \quad (215)$$

$$T_o^2 = \frac{m_h^2 - 8Bv^2}{4D} \quad (216)$$

$$B = \frac{3}{64\pi^2 v^4} (2m_W^4 + m_Z^4 - 4m_t^4) \quad (217)$$

$$\lambda(T) = \lambda - \frac{3}{16\pi^2 v^4} \left(2m_W^4 \log \frac{m_W^2}{A_B T^2} + m_Z^4 \log \frac{m_Z^2}{A_B T^2} - 4m_t^4 \log \frac{m_t^2}{A_F T^2} \right) \quad (218)$$

where $\log A_B = \log a_b - 3/2$ and $\log A_F = \log a_F - 3/2$, and a_B, a_F are given in (174) and (200). All the masses which appear in the definition of the coefficients, Eqs. (214) to (218), are the physical masses, *i.e.* the masses at the zero temperature minimum. The peculiar form of the potential, as given by Eq. (213), will be useful to study the associated phase transition, as we will see in subsequent sections.

4 Cosmological phase transitions

All cosmological applications of field theories are based on the theory of phase transitions at finite temperature, that we will briefly describe throughout this

section. The main point here is that at finite temperature, the equilibrium value of the scalar field ϕ , $\langle\phi(T)\rangle$, does not correspond to the minimum of the effective potential $V_{\text{eff}}^{T=0}(\phi)$, but to the minimum of the finite temperature effective potential $V_{\text{eff}}^\beta(\phi)$, as given by (159). Thus, even if the minimum of $V_{\text{eff}}^{T=0}(\phi)$ occurs at $\langle\phi\rangle = \sigma \neq 0$, very often, for sufficiently large temperatures, the minimum of $V_{\text{eff}}^\beta(\phi)$ occurs at $\langle\phi(T)\rangle = 0$: this phenomenon is known as **symmetry restoration** at high temperature, and gives rise to the phase transition from $\phi(T) = 0$ to $\phi = \sigma$. It was discovered by Kirzhnits²⁷ in the context of the electroweak theory (symmetry breaking between weak and electromagnetic interactions occurs when the universe cools down to a critical temperature $T_c \sim 10^2 \text{ GeV}$) and subsequently confirmed and developed by other authors^{28,15,16,29}.

The cosmological scenario can be drawn as follows: In the theory of the hot big bang, the universe is initially at very high temperature and, depending on the function $V_{\text{eff}}^\beta(\phi)$, it can be in the **symmetric phase** $\langle\phi(T)\rangle = 0$, *i.e.* $\phi = 0$ can be the stable absolute minimum. At some critical temperature T_c the minimum at $\phi = 0$ becomes metastable and the phase transition may proceed. The phase transition may be **first** or **second** order. First-order phase transitions have supercooled (out of equilibrium) symmetric states when the temperature decreases and are of use for baryogenesis purposes. Second-order phase transitions are used in the so-called new inflationary models³⁰. We will illustrate these kinds of phase transitions with very simple examples.

4.1 First and second order phase transitions

We will illustrate the difference between **first** and **second** order phase transitions by considering first the simple example of a potential^f described by the function,

$$V(\phi, T) = D(T^2 - T_o^2)\phi^2 + \frac{\lambda(T)}{4}\phi^4 \quad (219)$$

where D and T_o^2 are constant terms and λ is a slowly varying function of T ^g. A quick glance at (174) and (200) shows that the potential (219) can be part of the one-loop finite temperature effective potential in field theories.

At zero temperature, the potential has a negative mass-squared term, which indicates that the state $\phi = 0$ is unstable, and the energetically favored state corresponds to the minimum at $\phi(0) = \pm\sqrt{\frac{2D}{\lambda}}T_o$, where the symmetry $\phi \leftrightarrow -\phi$ of the original theory is spontaneously broken.

^fThe ϕ independent terms in (219), *i.e.* $V(0, T)$, are not explicitly considered.

^gThe T dependence of λ will often be neglected in this section.

The curvature of the finite temperature potential (219) is now T -dependent,

$$m^2(\phi, T) = 3\lambda\phi^2 + 2D(T^2 - T_o^2) \quad (220)$$

and its stationary points, *i.e.* solutions to $dV(\phi, T)/d\phi = 0$, given by,

$$\begin{aligned} \phi(T) &= 0 \\ \text{and} & \\ \phi(T) &= \sqrt{\frac{2D(T_o^2 - T^2)}{\lambda(T)}} \end{aligned} \quad (221)$$

Therefore the critical temperature is given by T_o . At $T > T_o$, $m^2(0, T) > 0$ and the origin $\phi = 0$ is a minimum. At the same time only the solution $\phi = 0$ in (221) does exist. At $T = T_o$, $m^2(0, T_o) = 0$ and both solutions in (221) collapse at $\phi = 0$. The potential (219) becomes,

$$V(\phi, T_o) = \frac{\lambda(T_o)}{4}\phi^4 \quad (222)$$

At $T < T_o$, $m^2(0, T) < 0$ and the origin becomes a maximum. Simultaneously, the solution $\phi(T) \neq 0$ does appear in (221). This phase transition is called of **second order**, because there is no barrier between the symmetric and broken phases. Actually, when the broken phase is formed, the origin (symmetric phase) becomes a maximum. The phase transition may be achieved by a thermal fluctuation for a field located at the origin.

However, in many interesting theories there is a **barrier** between the symmetric and broken phases. This is characteristic of **first order** phase transitions. A typical example is provided by the potential ^{*h*},

$$V(\phi, T) = D(T^2 - T_o^2)\phi^2 - ET\phi^3 + \frac{\lambda(T)}{4}\phi^4 \quad (223)$$

where, as before, D , T_0 and E are T independent coefficients, and λ is a slowly varying T -dependent function. Notice that the difference between (223) and (219) is the cubic term with coefficient E . This term can be provided by the contribution to the effective potential of bosonic fields (174). The behaviour of (223) for the different temperatures is reviewed in Refs.^{12,31}. At $T > T_1$ the only minimum is at $\phi = 0$. At $T = T_1$

$$T_1^2 = \frac{8\lambda(T_1)DT_o^2}{8\lambda(T_1)D - 9E^2} \quad (224)$$

^{*h*}See, *e.g.* the one-loop effective potential for the Standard Model, Eq. (90).

a local minimum at $\phi(T) \neq 0$ appears as an inflection point. The value of the field ϕ at $T = T_1$ is,

$$\langle \phi(T_1) \rangle = \frac{3ET_1}{2\lambda(T_1)} \quad (225)$$

A barrier between the latter and the minimum at $\phi = 0$ starts to develop at lower temperatures. Then the point (225) splits into a maximum

$$\phi_M(T) = \frac{3ET}{2\lambda(T)} - \frac{1}{2\lambda(T)} \sqrt{9E^2T^2 - 8\lambda(T)D(T^2 - T_o^2)} \quad (226)$$

and a local minimum

$$\phi_m(T) = \frac{3ET}{2\lambda(T)} + \frac{1}{2\lambda(T)} \sqrt{9E^2T^2 - 8\lambda(T)D(T^2 - T_o^2)} \quad (227)$$

At a given temperature $T = T_c$

$$T_c^2 = \frac{\lambda(T_c)DT_o^2}{\lambda(T_c)D - E^2} \quad (228)$$

the origin and the minimum (227) become degenerate. From (226) and (227) we find that

$$\phi_M(T_c) = \frac{ET_c}{\lambda(T_c)} \quad (229)$$

and

$$\phi_m(T_c) = \frac{2ET_c}{\lambda(T_c)} \quad (230)$$

For $T < T_c$ the minimum at $\phi = 0$ becomes metastable and the minimum at $\phi_m(T) \neq 0$ becomes the global one. At $T = T_o$ the barrier disappears, the origin becomes a maximum

$$\phi_M(T_o) = 0 \quad (231)$$

and the second minimum becomes equal to

$$\phi_m(T_o) = \frac{3ET_o}{\lambda(T_o)} \quad (232)$$

The phase transition starts at $T = T_c$ by tunneling. However, if the barrier is high enough the tunneling effect is very small and the phase transition does effectively start at a temperature $T_c > T_t > T_o$. In some models T_o can be equal to zero. The details of the phase transition depend therefore on the process of tunneling from the false to the global minimum. These details will be studied in the rest of this section.

4.2 Thermal tunneling

The transition from the false to the true vacuum proceeds via **thermal tunneling** at finite temperature. It can be understood in terms of formation of bubbles of the broken phase in the sea of the symmetric phase. Once this has happened, the bubble spreads throughout the universe converting false vacuum into true one.

The tunneling rate^{32,33,34} is computed by using the rules of field theory at finite temperature³⁵. In the previous section we defined the critical temperature T_c as the temperature at which the two minima of the potential $V(\phi, T)$ have the same depth. However, tunneling with formation of bubbles of the field ϕ corresponding to the second minimum starts somewhat later, and goes sufficiently fast to fill the universe with bubbles of the new phase only at some lower temperature T_t when the corresponding euclidean action $S_E = S_3/T$ suppressing the tunneling becomes $\mathcal{O}(130 - 140)$ ^{36,37,12}, as we will see in the next section.

We will use as prototype the potential of Eq. (223) which can trigger, as we showed in this section, a first order phase transition. In this case the false minimum is $\phi = 0$, and the value of the potential at the origin is zero, $V(0, T) = 0$. The tunneling probability per unit time per unit volume is given by³⁵

$$\frac{\Gamma}{\nu} \sim A(T)e^{-S_3/T} \quad (233)$$

In (233) the prefactor $A(T)$ is roughly of $\mathcal{O}(T^4)$ while S_3 is the three-dimensional euclidean action defined as

$$S_3 = \int d^3x \left[\frac{1}{2} (\vec{\nabla}\phi)^2 + V(\phi, T) \right]. \quad (234)$$

At very high temperature the **bounce** solution has $O(3)$ symmetry³⁵ and the euclidean action is then simplified to,

$$S_3 = 4\pi \int_0^\infty r^2 dr \left[\frac{1}{2} \left(\frac{d\phi}{dr} \right)^2 + V(\phi(r), T) \right] \quad (235)$$

where $r^2 = \vec{x}^2$, and the euclidean equation of motion yields,

$$\frac{d^2\phi}{dr^2} + \frac{2}{r} \frac{d\phi}{dr} = V'(\phi, T) \quad (236)$$

with the boundary conditions

$$\lim_{r \rightarrow \infty} \phi(r) = 0 \quad (237)$$

$$\left. \frac{d\phi}{dr} \right|_{r=0} = 0 \quad (238)$$

From here on we will follow the discussion in Ref. ¹². Let us take $\phi = 0$ outside a bubble. Then (235), which is also the surplus free energy of a true vacuum bubble, can be written as

$$S_3 = 4\pi \int_0^R r^2 dr \left[\frac{1}{2} \left(\frac{d\phi}{dr} \right)^2 + V(\phi(r), T) \right] \quad (239)$$

where R is the bubble radius. There are two contributions to (239): a surface term F_S , coming from the derivative term in (239), and a volume term F_V , coming from the second term in (239). They scale like,

$$S_3 \sim 2\pi R^2 \left(\frac{\delta\phi}{\delta R} \right)^2 \delta R + \frac{4\pi R^3 \langle V \rangle}{3} \quad (240)$$

where δR is the thickness of the bubble wall, $\delta\phi = \phi_m$ and $\langle V \rangle$ is the average of the potential inside the bubble.

For temperatures just below T_c , the height of the barrier $V(\phi_M, T)$ is large compared to the depth of the potential at the minimum, $-V(\phi_m, T)$. In that case, the solution of minimal action corresponds to minimizing the contribution to F_V coming from the region $\phi = \phi_M$. This amounts to a very small bubble wall $\delta R/R \ll 1$ and so a very quick change of the field from $\phi = 0$ outside the bubble to $\phi = \phi_m$ inside the bubble. Therefore, the first formed bubbles after T_c are **thin wall** bubbles.

Subsequently, when the temperature drops towards T_o the height of the barrier $V(\phi_M, T)$ becomes small as compared with the depth of the potential at the minimum $-V(\phi_m, T)$. In that case the contribution to F_V from the region $\phi = \phi_M$ is negligible, and the minimal action corresponds to minimizing the surface term F_S . This amounts to a configuration where δR is as large as possible, *i.e.* $\delta R/R = \mathcal{O}(1)$: **thick wall** bubbles. So whether the phase transition proceeds through thin or thick wall bubbles depends on how large the bubble nucleation rate (233) is, or how small S_3 is, before thick bubbles are energetically favoured.

For the potential (223) an analytic formula has been obtained in Ref. ³¹ without assuming the thin wall approximation. It is given by,

$$\frac{S_3}{T} = \frac{13.72}{E^2} \left[D \left(1 - \frac{T_o^2}{T^2} \right) \right]^{3/2} f \left[\frac{\lambda(T)D}{E^2} \left(1 - \frac{T_o^2}{T^2} \right) \right] \quad (241)$$

$$f(x) = 1 + \frac{x}{4} \left[1 + \frac{2.4}{1-x} + \frac{0.26}{(1-x)^2} \right] \quad (242)$$

The case of two fields is extremely more complicated. In particular the two-Higgs situation in the supersymmetric standard theory has been recently solved in Ref. ³⁸. The connection between zero temperature and finite temperature tunneling is manifest. In particular at temperatures much less than the inverse radius the ($T = 0$) $O(4)$ solution has the least action. This can happen for theories with a supercooled symmetric phase: for instance in the presence of a barrier that does not disappear when the temperature drops to zero. At temperatures much larger than the inverse radius, the $O(3)$ solution has the least action.

4.3 Bubble nucleation

In the previous subsection we have established the free energy and the critical radius of a bubble large enough to grow after formation. The subsequent progress of the phase transition depends on the ratio of the rate of production of bubbles of true vacuum, as given by (233), over the expansion rate of the universe. For example if the former remains always smaller than the latter, then the state will be trapped in the supercooled false vacuum. Otherwise the phase transition will start at some temperature T_t by **bubble nucleation**. The probability of bubble formation per unit time per unit volume is given by (233) where $B(T) = S_3(T)/T$, $A(T) = \omega T^4$, where the parameter ω will be taken of $\mathcal{O}(1)$.

Since the progress of the phase transition should depend on the expansion rate of the universe, we have to describe the universe at temperatures close to the electroweak phase transition. A homogeneous and isotropic (flat) universe is described by a Robertson-Walker metric which, in comoving coordinates, is given by $ds^2 = dt^2 - a(t)^2 (dr^2 + r^2 d\Omega^2)$, where $a(t)$ is the scale factor of the universe. The universe expansion is governed by the equation

$$\left(\frac{\dot{a}}{a} \right)^2 = \frac{8\pi}{3M_{Pl}^2} \rho \quad (243)$$

where M_{Pl} is the Planck mass, and ρ is the energy density. For temperatures $T \sim 10^2 \text{ GeV}$ the universe is radiation dominated, and its energy density is given by,

$$\rho = \frac{\pi^2}{30} g(T) T^4 \quad (244)$$

where $g(T) = g_B(T) + \frac{7}{8} g_F(T)$, and $g_B(T)$ ($g_F(T)$) is the effective number of bosonic (fermionic) degrees of freedom at the temperature T . For the stan-

standard model we have $g^{SM} = 106.75$ which can be considered as temperature independent.

The equation of motion (243) can be solved, and assuming an adiabatic expansion of the universe, $a(T_1)T_1 = a(T_2)T_2$, one obtains the following relationship,

$$t = \zeta \frac{M_{Pl}}{T^2} \quad (245)$$

where $\zeta = \frac{1}{4\pi} \sqrt{\frac{45}{\pi g}} \sim 3 \times 10^{-2}$. Using (245) the horizon volume is given by

$$V_H(t) = 8\zeta^3 \frac{M_{Pl}^3}{T^6} \quad (246)$$

The onset of nucleation happens at a temperature T_t such that **the probability for a single bubble to be nucleated within one horizon volume is ~ 1** , i.e. ³⁸

$$\int_{T_t}^{\infty} \frac{dT}{T} \left(\frac{2\zeta M_{Pl}}{T} \right)^4 \exp\{-S_3(T)/T\} = \mathcal{O}(1) . \quad (247)$$

which implies numerically,

$$B(T_t) \sim 137 + \log \frac{10^2 E^2}{\lambda D} + 4 \log \frac{100 \text{ GeV}}{T_t} \quad (248)$$

where we have normalized $T_t \sim 100 \text{ GeV}$ and $E^2/(\lambda D) \sim 10^{-2}$ which are typical values which will be obtained in the standard model of electroweak interactions.

5 Baryogenesis at phase transitions

There are two essential problems to be understood related with the baryon number of the universe:

i) There is no evidence of antimatter in the universe. In fact, there is no antimatter in the solar system, and only \bar{p} in cosmic rays. However antiprotons can be produced as secondaries in collisions ($pp \rightarrow 3p + \bar{p}$) at a rate similar to the observed one. Numerically, $\frac{n_{\bar{p}}}{n_p} \sim 3 \times 10^{-4}$, and $\frac{n_{^4He}}{n_{^4He}} \sim 10^{-5}$. We can conclude that $n_B \gg n_{\bar{B}}$, so $n_{\Delta B} \equiv n_B - n_{\bar{B}} \sim n_B$.

ii) The second problem is to understand the origin of

$$\eta \equiv \frac{n_B}{n_\gamma} \sim (0.3 - 1.0) \times 10^{-9} \quad (249)$$

today. This parameter is essential for primordial nucleosynthesis³⁹. η may not have changed since nucleosynthesis. At these energy scales (~ 1 MeV) baryon number is conserved if there are no processes which would have produced entropy to change the photon number. We can easily estimate from η the baryon to entropy ratio by using

$$s = \frac{\pi^4}{45\zeta(3)} 3.91 n_\gamma = 7.04 n_\gamma \quad (250)$$

and the range (249).

In the standard cosmological model there is no explanation for the smallness of the ratio (249) if we start from $n_{\Delta B} = 0$. An initial asymmetry has to be imposed by hand as an initial condition (which violates any naturalness principle) or has to be dynamically generated at phase transitions, which is the way we will explore all along this section.

5.1 Conditions for baryogenesis

As we have seen in the previous subsection the universe was initially baryon symmetric ($n_B \simeq n_{\bar{B}}$) although the matter-antimatter asymmetry appears to be large today ($n_{\Delta B} \simeq n_B \gg n_{\bar{B}}$). In the standard cosmological model there is no explanation for the value of η consistent with nucleosynthesis, Eq. (249), and it has to be imposed by hand as an initial condition. However, it was suggested by Sakharov long ago⁴⁰ that a tiny $n_{\Delta B}$ might have been produced in the early universe leading, after $p\bar{p}$ annihilations, to (249). The three ingredients necessary for baryogenesis are:

B-nonconserving interactions

This condition is obvious since we want to start with a baryon symmetric universe ($\Delta B = 0$) and evolve it to a universe where $\Delta B \neq 0$. B-nonconserving interactions might mediate proton decay; in that case the phenomenological constraints are provided by the proton lifetime measurements⁴¹ $\tau_p \gtrsim 10^{32} yr$.

C and CP violation

The action of C (charge conjugation) and CP (combined action of charge conjugation and parity) interchanges particles with antiparticles, changing therefore the sign of B . For instance if we describe spin- $\frac{1}{2}$ fermions by two-component fields of definite chirality (left-handed fields ψ_L and right-handed

fields ψ_R) the action of C and CP over them is given by

$$\begin{aligned}
P & : \psi_L \longrightarrow \psi_R, \quad \psi_R \longrightarrow \psi_L \\
C & : \psi_L \longrightarrow \psi_L^C \equiv \sigma_2 \psi_R^*, \quad \psi_R \longrightarrow \psi_R^C \equiv -\sigma_2 \psi_L^* \\
CP & : \psi_L \longrightarrow \psi_R^C, \quad \psi_R \longrightarrow \psi_L^C
\end{aligned} \tag{251}$$

If the universe is initially matter-antimatter symmetric, and without a preferred direction of time as in the standard cosmological model, it is represented by a C and CP invariant state, $|\phi_o\rangle$, with $B = 0$. If C and CP were conserved, *i.e.* $[C, H] = [CP, H] = 0$, H being the hamiltonian, then the state of the universe at a later time t , $|\phi(t)\rangle = e^{iHt}|\phi_o\rangle$ would be C and CP invariant and, therefore, baryon number conserving, $\Delta B = 0$. The only way to generate a net $\Delta B \neq 0$ is to have C and CP violating interactions.

Departure from thermal equilibrium

If all particles in the universe remained in thermal equilibrium, then no direction for time would be defined and CPT invariance would prevent the appearance of any baryon excess, rendering CP violating interactions irrelevant⁴².

A particle species is in thermal equilibrium if all its reaction rates, Γ , are much faster than the expansion rate of the universe, H . On the other hand a departure from thermal equilibrium is expected whenever a rate crucial for maintaining it is less than the expansion rate ($\Gamma < H$). Deviation from thermal equilibrium cannot occur in a homogeneous isotropic universe containing only massless species: massive species are needed in general for such deviations to occur.

5.2 Baryogenesis at the electroweak phase transitions

It has been recently realized^{43,44} that the three Sakharov's conditions for baryogenesis can be fulfilled at the electroweak phase transition:

- Baryonic charge non-conservation was discovered by 't Hooft⁴⁵. In fact baryon and lepton number are conserved anomalous global symmetries in the Standard Model. They are violated by non-perturbative effects.
- CP violation can be generated in the Standard Model from phases in the fermion mass matrix, Cabibbo, Kobayashi, Maskawa (CKM) phases⁴⁶. This effect is much too small to explain the observed baryon to entropy ratio. However, in extensions of the Standard Model as the minimal supersymmetric standard model (MSSM), a sizeable CP violation can happen through an extended Higgs sector.

- The out of equilibrium condition can be achieved, if the phase transition is strong enough first order, in the bubble walls. In that case the B-violating interactions are out of equilibrium in the bubble walls and a net B-number can be generated during the phase transition⁴⁴.

Baryon and lepton number violation in the electroweak theory

Violation of baryon and lepton number in the electroweak theory is a very striking phenomenon. Classically, baryonic and leptonic currents are conserved in the electroweak theory. However, that conservation is spoiled by quantum corrections through the chiral anomaly associated with triangle fermionic loop in external gauge fields. The calculation gives,

$$\partial_\mu j_B^\mu = \partial_\mu j_L^\mu = N_f \left(\frac{g^2}{32\pi^2} W\widetilde{W} - \frac{g'^2}{32\pi^2} Y\widetilde{Y} \right) \quad (252)$$

where N_f is the number of fermion generations, $W_{\mu\nu}$ and $Y_{\mu\nu}$ are the gauge field strength tensors for $SU(2)$ and $U(1)_Y$, respectively, and the tilde means the dual tensor.

A very important feature of (252) is that the difference $B - L$ is strictly conserved, and so only the sum $B + L$ is anomalous and can be violated. Another feature is that fluctuations of the gauge field strengths can lead to fluctuations of the corresponding value of $B + L$. The product of gauge field strengths on the right hand side of Eq. (252) can be written as four-divergences, $W\widetilde{W} = \partial_\mu k_W^\mu$, $Y\widetilde{Y} = \partial_\mu k_Y^\mu$, where

$$\begin{aligned} k_Y^\mu &= \epsilon^{\mu\nu\alpha\beta} Y_{\nu\alpha} Y_\beta \\ k_W^\mu &= \epsilon^{\mu\nu\alpha\beta} \left(W_{\nu\alpha}^a W_\beta^a - \frac{g}{3} \epsilon_{abc} W_\nu^a W_\alpha^b W_\beta^c \right) \end{aligned} \quad (253)$$

and W_μ , Y_μ are the gauge fields of $SU(2)$ and $U(1)_Y$, respectively. In general total derivatives are unobservable because they can be integrated by parts and drop from the integrals. This is true for the terms in the four-vectors (253) proportional to the field strengths $W_{\mu\nu}$ and $Y_{\mu\nu}$. This means that for the abelian subgroup $U(1)_Y$ the current non conservation induced by quantum effects becomes non observable. However this is not mandatory for gauge fields, for which the integral can be nonzero. Hence only for non-abelian groups can the current non conservation induced by quantum effects become observable. In particular one can write $\Delta B = \Delta L = N_f \Delta N_{CS}$, where N_{CS} is the so-called Chern-Simons number characterizing the topology of the gauge field configuration,

$$N_{CS} = \frac{g^2}{32\pi^2} \int d^3x \epsilon^{ijk} \left(W_{ij}^a W_k^a - \frac{g}{3} \epsilon_{abc} W_i^a W_j^b W_k^c \right) \quad (254)$$

Note that though N_{CS} is not gauge invariant, its variation ΔN_{CS} is.

We want to compute now ΔB between an initial and a final configuration of gauge fields. We are considering vacuum field strength tensors $W_{\mu\nu}$ which vanish. The corresponding potentials are not necessarily zero but can be represented by purely gauge fields,

$$W_\mu = -\frac{i}{g}U(x)\partial_\mu U^{-1}(x) \quad (255)$$

There are two classes of gauge transformations keeping $W_{\mu\nu} = 0$:

- Continuous transformations of the potentials yielding $\Delta N_{CS} = 0$.
- If one tries to generate $\Delta N_{CS} \neq 0$ by a continuous variation of the potentials, then one has to enter a region where $W_{\mu\nu} \neq 0$. This means that vacuum states with different topological charges are separated by potential barriers.

The probability of barrier penetration can be calculated using the quasi-classical approximation³². In euclidean space time, the trajectory in field space configuration which connects two vacua differing by a unit of topological charge is called instanton. The euclidean action evaluated at this trajectory gives the probability for barrier penetration as $\Gamma \sim \exp\left(-\frac{4\pi}{\alpha_W}\right) \sim 10^{-162}$, where $\alpha_W = g^2/4\pi$. This number is so small that the calculation of the pre-exponential is unnecessary and the probability for barrier penetration is essentially zero.

Baryon violation at finite temperature: sphalerons

However, in a system with non zero temperature a particle may classically go over the barrier with a probability determined by the Boltzmann exponent, as we have seen.

What we have is a potential which depends on the gauge field configuration W_μ . This potential has an infinite number of degenerate minima, labeled as Ω_n . These minima are characterized by different values of the Chern-Simons number. The minimum Ω_0 corresponds to the configuration $W_\mu = 0$ and we can take conventionally the value of the potential at this point to be zero. Other minima have gauge fields given by (255). In the temporal gauge $W_0 = 0$, the gauge transformation U must be time independent (since we are considering gauge configurations with $W_{\mu\nu} = 0$), *i.e.* $U = U(\vec{x})$, and so functions U define maps,

$$U : S^3 \longrightarrow SU(2)$$

All the minima with $W_{\mu\nu} = 0$ have equally zero potential energy, but those defined by a map $U(\vec{x})$ with nonzero Chern-Simons number

$$n[U] = \frac{1}{24\pi^2} \int d^3x \epsilon^{ijk} \text{Tr}(U \partial_i U^{-1} U \partial_j U^{-1} U \partial_k U^{-1}) \quad (256)$$

correspond to degenerate minima in the configuration space with non-zero baryon and lepton number.

Degenerate minima are separated by a potential barrier. The field configuration at the top of the barrier is called **sphaleron**, which is a *static unstable* solution to the classic equations of motion⁴⁷. The sphaleron solution has been explicitly computed in Ref.⁴⁷ for the case of zero Weinberg angle, (*i.e.* neglecting terms $\mathcal{O}(g')$), and for an arbitrary value of $\sin^2 \theta_W$ in Ref.⁴⁸.

An ansatz for the sphaleron solution for the case of zero Weinberg angle was given (for the zero temperature potential) in Ref.⁴⁷, for the Standard Model with a single Higgs doublet, as,

$$W_i^a \sigma^a dx^i = -\frac{2i}{g} f(\xi) dU U^{-1} \quad (257)$$

for the gauge field, and

$$\Phi = \frac{v}{\sqrt{2}} h(\xi) U \begin{pmatrix} 0 \\ 1 \end{pmatrix} \quad (258)$$

for the Higgs field, where the gauge transformation U is taken to be,

$$U = \frac{1}{r} \begin{pmatrix} z & x + iy \\ -x + iy & z \end{pmatrix} \quad (259)$$

and we have introduced the dimensionless radial distance $\xi = gvr$.

Using the ansatz (257), (258) and (259) the field equations reduce to,

$$\begin{aligned} \xi^2 \frac{d^2 f}{d\xi^2} &= 2f(1-f)(1-2f) - \frac{\xi^2}{4} h^2(1-f) \\ \frac{d}{d\xi} \left(\xi^2 \frac{dh}{d\xi} \right) &= 2h(1-f)^2 + \frac{\lambda}{g^2} \xi^2 (h^2 - 1)h \end{aligned} \quad (260)$$

with the boundary conditions, $f(0) = h(0) = 0$ and $f(\infty) = h(\infty) = 1$. The energy functional becomes then,

$$\begin{aligned} E &= \frac{4\pi v}{g} \int_0^\infty \left\{ 4 \left(\frac{df}{d\xi} \right)^2 + \frac{8}{\xi^2} [f(1-f)]^2 + \frac{1}{2} \xi^2 \left(\frac{dh}{d\xi} \right)^2 \right. \\ &+ \left. [h(1-f)]^2 + \frac{1}{4} \left(\frac{\lambda}{g^2} \right) \xi^2 (h^2 - 1)^2 \right\} d\xi \end{aligned} \quad (261)$$

The solution to Eqs. (260) has to be found numerically. The solutions depend on the gauge and quartic couplings, g and λ . Once replaced into the energy functional (261) they give the sphaleron energy which is the height of the barrier between different degenerate minima. It is customary to write the solution as,

$$E_{\text{sph}} = \frac{2m_W}{\alpha_W} B(\lambda/g^2) \quad (262)$$

where B is the constant which requires numerical evaluation. For the standard model with a single Higgs doublet this parameter ranges from $B(0) = 1.5$ to $B(\infty) = 2.7$. A fit valid for values of the Higgs mass $25 \text{ GeV} \leq m_h \leq 250 \text{ GeV}$ can be written as,

$$B(x) = 1.58 + 0.32x - 0.05x^2 \quad (263)$$

where $x = m_h/m_W$.

The previous calculation of the sphaleron energy was performed at zero temperature. The sphaleron at finite temperature was computed in Ref. ^{49,50}. Its energy follows the approximate scaling law, $E_{\text{sph}}(T) = E_{\text{sph}} \langle \phi(T) \rangle / \langle \phi(0) \rangle$ which, using (262), can be written as,

$$E_{\text{sph}}(T) = \frac{2m_W(T)}{\alpha_W} B(\lambda/g^2) \quad (264)$$

where $m_W(T) = \frac{1}{2}g \langle \phi(T) \rangle$

Baryon violation rate at $T > T_c$

The calculation of the baryon violation rate at $T > T_c$, *i.e.* in the symmetric phase, is very different from that in the broken phase, that will be reviewed in the next section. In the symmetric phase, at $\phi = 0$, the perturbation theory is spoiled by infrared divergences, and so we cannot rely upon perturbative calculations to compute the baryon violation rate in this phase. In fact, the infrared divergences are cut off by the non-perturbative generation of a **magnetic mass**, $m_M \sim \alpha_W T$, *i.e.* a **magnetic screening length** $\xi_M \sim (\alpha_W T)^{-1}$. The rate of baryon violation per unit time and unit volume Γ does not contain any exponential Boltzmann factor ^{*i*}. The pre-exponential can be computed from dimensional grounds ⁵¹ as

$$\Gamma = k(\alpha_W T)^4 \quad (265)$$

where the coefficient k has been evaluated numerically in Ref. ⁵² with the result ^{*j*} $0.1 \lesssim k \lesssim 1.0$.

^{*i*}It would disappear from (233) in the limit $T \rightarrow \infty$.

^{*j*}In fact recent lattice computations ⁵³ seem to provide an extra factor in (265) as $k'\alpha_W$ which is roughly speaking $\mathcal{O}(1)$.

Baryon violation rate at $T < T_c$

After the phase transition, the calculation of baryon violation rate can be done using the semiclassical approximations given by Eq. (233). The rate per unit time and unit volume for fluctuations between neighboring minima contains a Boltzmann suppression factor $\exp(-E_{\text{sph}}(T)/T)$, where $E_{\text{sph}}(T)$ is given by (264), and a pre-factor containing the determinant of all zero and non-zero modes. The prefactor was computed in Ref. ⁵⁴ as

$$\Gamma \sim 2.8 \times 10^5 T^4 \left(\frac{\alpha_W}{4\pi} \right)^4 \kappa \frac{\zeta^7}{B^7} e^{-\zeta} \quad (266)$$

where we have defined $\zeta(T) = E_{\text{sph}}(T)/T$, the coefficient B is the function of λ/g^2 defined in (263) and κ is the functional determinant associated with fluctuations about the sphaleron. It has been estimated ³⁷ to be in the range, $10^{-4} \lesssim \kappa \lesssim 10^{-1}$.

The equation describing the dilution S of the baryon asymmetry in the anomalous electroweak processes reads ⁵⁵

$$\frac{\partial S}{\partial t} = -V_B(t)S \quad (267)$$

where $V_B(t)$ is the rate of the baryon number non-conserving processes. Assuming T is constant during the phase transition the integration of (267) yields $S = e^{-X}$ and $X = \frac{13}{2} N_f \frac{\Gamma}{T^3} t$. Using now (266) and (245) we can write the exponent X as, $X \sim 10^{10} \kappa \zeta^7 e^{-\zeta}$, where we have taken the values of the parameters, $B = 1.87$, $\alpha_W = 0.0336$, $N_f = 3$, $T_c \sim 10^2 \text{ GeV}$. Imposing now the condition $S \gtrsim 10^{-5}$, or $X \lesssim 10$, leads to the condition on $\zeta(T_c)$,

$$\zeta(T_c) \gtrsim 7 \log \zeta(T_c) + 9 \log 10 + \log \kappa \quad (268)$$

Now, taking κ at its upper bound, $\kappa = 10^{-1}$, we obtain from (268) the bound ⁵⁶

$$\frac{E_{\text{sph}}(T_c)}{T_c} \gtrsim 45, \quad (269)$$

and using the lower bound, $\kappa = 10^{-4}$ we obtain,

$$\frac{E_{\text{sph}}(T_c)}{T_c} \gtrsim 37, \quad (270)$$

Eq. (269) is the usual bound used to test different theories while Eq. (270) gives an idea on how much can one move away from the bound (269), *i.e.* the uncertainty on the bound (269).

The bounds (269) and (270) can be translated into bounds on $\phi(T_c)/T_c$. Using the relation (264) we can write

$$\frac{\phi(T_c)}{T_c} = \frac{g}{4\pi B} \frac{E_{\text{sph}}(T_c)}{T_c} \sim \frac{1}{36} \frac{E_{\text{sph}}(T_c)}{T_c} \quad (271)$$

where we have used the previous values of the parameters. The bound (269) translates into

$$\frac{\phi(T_c)}{T_c} \gtrsim 1.3 \quad (272)$$

while the bound (270) translates into,

$$\frac{\phi(T_c)}{T_c} \gtrsim 1.0 \quad (273)$$

These bounds, Eqs. (272) and (269), require that the phase transition is strong enough first order. In fact for a second order phase transition, $\phi(T_c) \simeq 0$ and any previously generated baryon asymmetry would be washed out during the phase transition. For the case of the Standard Model the previous bounds translate into a bound on the Higgs mass, as we will see.

6 On the validity of the perturbative expansion

The approach of Ref. ¹⁶ to the finite temperature effective potential relied on the observation that **symmetry restoration implies that ordinary perturbation theory must break down at high temperature**. In fact, otherwise perturbation theory should hold and, since the tree level potential is temperature independent, radiative corrections (which are temperature dependent) should be unable to restore the symmetry. We will see that the failure of perturbative expansion is intimately linked to the appearance of infrared divergences for the zero Matsubara modes of bosonic degrees of freedom. This just means that the usual perturbative expansion in powers of the coupling constant fails at temperatures beyond the critical temperature. It has to be replaced by an improved perturbative expansion where an infinite number of diagrams are resummed at each order in the new expansion. We will review the actual situation in this section.

6.1 The breakdown of perturbative expansion

We will examine the simplest model of one self-interacting real scalar field, described by a lagrangian with a squared-mass term, m^2 and a quartic coupling λ . We will use now power counting arguments to investigate the high

temperature behaviour of higher loop diagrams contributing to the effective potential^{16,57,58}. After rescaling all loop momenta and energies by T , a loop amplitude with superficial divergence D takes the form, $T^D f(m/T)$. If there are no infrared divergences when $m/T \rightarrow 0$, then the loop goes like T^D . For instance the diagram contributing to the self-energy of Fig. 5 is quadratically

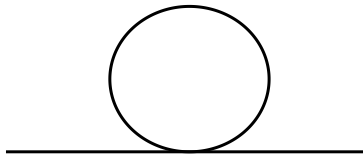


Figure 5: One-loop contribution to the self-energy for the scalar theory.

divergent ($D = 2$), and so behaves like λT^2 . For $D \leq 0$, there are infrared divergences associated to the zero modes of bosonic propagators in the imaginary time formalism [$n = 0$ in (147)] and the only T dependence comes from the T in front of the loop integral in (147). Then every logarithmically divergent or convergent loop contributes a factor of T . For instance the diagram contributing to the self-energy in Fig. 6 contains two logarithmically divergent

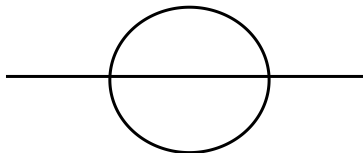


Figure 6: Two-loop contribution to the self-energy for the scalar theory.

loops and so behaves like, $\lambda^2 T^2 = \lambda(\lambda T^2)$. It is clear that to a fixed order in the loop expansion the largest graphs are those with the maximum number of quadratically divergent loops. These diagrams are obtained from the diagram in Fig. 5 by adding n quadratically divergent loops on top of it, as shown in Fig. 7.

They behave as,

$$\lambda^{n+1} \frac{T^{2n+1}}{M^{2n-1}} = \lambda^2 \frac{T^3}{M} \left(\frac{\lambda T^2}{M^2} \right)^{n-1} \quad (274)$$

where M is the mass scale of the theory, and has been introduced to rescale

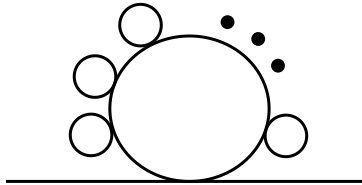


Figure 7: Daisy (n+1)-loop contribution to the self-energy for the scalar theory.

the powers of the temperature ^k. As was clear from Eq. (274), adding a quadratically divergent bubble to a propagator which is part of a logarithmically divergent or finite loop amounts to multiplying the diagram by

$$\alpha \equiv \lambda \frac{T^2}{M^2} \quad (275)$$

This means that for the one-loop approximation to be valid it is required that

$$\lambda \frac{T^2}{M^2} \ll 1$$

along with the usual requirement for the ordinary perturbation expansion

$$\lambda \ll 1$$

However at the critical temperature we have that $T_c \sim M/\sqrt{\lambda}$ [see Eqs. (219)-(220)]. Therefore **at the critical temperature the one-loop approximation is not valid** and higher loop diagrams where multiple quadratically divergent bubbles are inserted cannot be neglected. Daisy resummation⁵⁹ consists precisely to resum all powers of α and provides a theory where $m^2(\phi_c) \rightarrow m_{\text{eff}}^2 \equiv m^2(\phi_c) + \Pi$, where Π is the self-energy corresponding to the one-loop resummed diagrams to leading order in powers of the temperature T (e.g. $\sim T^2$). This method was pursued systematically by Parwani⁶⁰ and applied to the Standard Model by Arnold and Espinosa⁶¹.

What about the diagrams which are not considered in the **improved** expansion? The two-loop diagram of Fig. 6 is suppressed with respect to the diagram of Fig. 5 by λ . On the other hand the multiple loop diagram obtained

^kIn fact, the mass M has a different meaning for the improved and the unimproved theories, as we shall see. For the unimproved theory, M is the mass in the shifted lagrangian, $M^2 = m^2(\phi)$, while in the improved theory, M is given by the thermal mass.

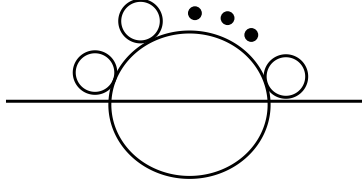


Figure 8: Non-daisy $(n+2)$ -loop contribution to the self-energy for the scalar theory.

from that of Fig. 6 by adding n quadratically divergent loops on top of it, see Fig. 8, behaves as

$$\lambda^{n+2} \frac{T^{2n+2}}{M^{2n}} = \lambda^{n+1} \frac{T^{2n+1}}{M^{2n-1}} \left(\lambda \frac{T}{M} \right) \quad (276)$$

and it is suppressed with respect to the multiple loop diagram of Eq. (274) by $\lambda T/M$ ^l. Therefore the validity of the improved expansion is guaranteed provided that,

$$\begin{aligned} \lambda &\ll 1 \\ \beta \equiv \lambda \frac{T}{M} &\ll 1 \end{aligned} \quad (277)$$

This simplified discussion can be done of course in more complicated field theories, as e.g. the Standard Model, with similar arguments⁶¹. We will now apply these results to two different models.

6.2 The scalar theory

In the case just considered of the scalar theory, the effective potential can be written in the one-loop daisy resummed approximation as

$$V(\phi, T) = \frac{1}{2} m_{\text{eff}}^2 \phi^2 - \frac{1}{12\pi} \left(m_{\text{eff}}^2 + \frac{1}{2} \lambda \phi^2 \right)^{3/2} + \frac{\lambda}{4!} \phi^4 + \dots \quad (278)$$

where $m_{\text{eff}}^2 \equiv m^2 + \frac{\lambda}{24} T^2$.

^lNon-daisy contributions to the self-energy are suppressed, with respect to daisy contributions, by $\mathcal{O}(\beta)$, where β is defined in (277). The corresponding contributions to the vacuum diagrams (*i.e.* effective potential) are suppressed by $\mathcal{O}(\beta^2)$ ⁵⁸.

The potential (278) apparently yields a first order phase transition⁶². However, the symmetry breaking minimum occurs when the three terms in the potential are similar. Then, at $T \sim T_c$, at the minimum

$$\phi \sim \sqrt{\lambda}T, \quad m_{\text{eff}}^2 \sim \lambda^2 T^2 \quad (279)$$

and then,

$$\beta \sim \lambda \frac{T}{m_{\text{eff}}} \sim \lambda \frac{T}{\lambda T} = \mathcal{O}(1) \quad (280)$$

which shows that the result of perturbation theory is fake⁶¹.

6.3 The Standard Model

In cases where there are gauge and/or Yukawa interactions, as the Standard Model case, the situation is completely different. The effective potential in the one-loop improved approximation, Eq. (213) can be written as

$$V(\phi, T) = \frac{1}{2} m_{\text{eff}}^2 \phi^2 - b g^3 \phi^3 T + \frac{\lambda}{4!} \phi^4 + \dots \quad (281)$$

where

$$b g^3 \phi^3 T \equiv [4M_W^3(\phi) + 2M_Z^3(\phi)] \frac{T}{12\pi} \equiv \left[\frac{1}{2} g^3 + (g^2 + g'^2)^{3/2} \right] \frac{T}{12\pi} \phi^3$$

and $m_{\text{eff}}^2 = m^2 + a g^2 T^2$, $a g^2$ denoting the contribution of gauge and Yukawa couplings to the one loop self-energy. We have only considered the contribution of transverse gauge bosons to the phase transition strength, and neglected that of the (screened) longitudinal gauge bosons.

Now again, symmetry breaking occurs when all terms are similar,

$$\phi \sim \frac{g^3}{\lambda} T, \quad m_{\text{eff}}^2 \sim \frac{g^6}{\lambda} T^2 \quad (282)$$

and the expansion parameter β ,

$$\beta_{\text{SM}} \sim g^2 \frac{T}{M_W(\phi)} \sim g \frac{T}{\phi} \sim \frac{\lambda}{g^2} \sim \frac{m_H^2}{m_W^2} \quad (283)$$

Therefore the validity of perturbation theory implies that $m_H \lesssim m_W$. This behaviour is supported by non-perturbative calculations⁶³.

7 Summary of physical results for the phase transition and constraints on the Higgs mass

7.1 Standard Model results

The effective potential for the Standard Model was analyzed in Eqs. (213), (281) in the one-loop approximation, including leading order plasma effects. In this approximation, the longitudinal components of the gauge bosons are screened by plasma effects while the transverse components remain unscreened. In this way a good approximation to the effective potential including these plasma effects is provided by Eq. (223), where the coefficient E is given by

$$E_{\text{SM}} = \frac{2}{3} \frac{2m_W^3 + m_Z^3}{4\pi v^3} \sim 9.5 \times 10^{-3} \quad (284)$$

Now we can use Eq. (230) and $m_h^2 = 2\lambda v^2$ to write,

$$\frac{\phi(T_c)}{T_c} \sim \frac{4Ev^2}{m_h^2} \quad (285)$$

In this way the bound (272) translates into the bound on the Higgs mass,

$$m_h \lesssim \sqrt{\frac{4E}{1.3}} \sim 42 \text{ GeV}. \quad (286)$$

The bound (286) is excluded by LEP measurements⁴¹, and so the Standard Model is unable to keep any previously generated baryon asymmetry. Including two-loop effects the bound is slightly increased to ~ 45 GeV⁶¹. Is it possible, in extensions of the Standard Model, to overcome this difficulty? We will see in the next section one typical example where the Standard Model is extended: the well motivated supersymmetric extension of the Standard Model.

7.2 MSSM results

Among the extensions of the Standard Model, the physically most motivated and phenomenologically most acceptable one is the Minimal Supersymmetric Standard Model. This model allows for extra CP-violating phases besides the Kobayashi-Maskawa one, which could help in generating the observed baryon asymmetry⁶⁴. It is then interesting to study whether in the MSSM the nature of the phase transition can be significantly modified with respect to the Standard Model.

In this section we extend the considerations of the previous section to the full parameter space, characterizing the Higgs sector of the MSSM^{65,66,67}.

The main tool for our study is the one-loop, daisy-improved finite-temperature effective potential of the MSSM, $V_{\text{eff}}(\phi, T)$. We are actually interested in the dependence of the potential on $\phi_1 \equiv \text{Re } H_1^0$ and $\phi_2 \equiv \text{Re } H_2^0$ only, where H_1^0 and H_2^0 are the neutral components of the Higgs doublets H_1 and H_2 , thus ϕ will stand for (ϕ_1, ϕ_2) . Working in the 't Hooft-Landau gauge and in the \overline{DR} -scheme, we can write

$$V_{\text{eff}}(\phi, T) = V_0(\phi) + V_1(\phi, 0) + \Delta V_1(\phi, T) + \Delta V_{\text{daisy}}(\phi, T) + V_2(\phi, T), \quad (287)$$

where

$$V_0(\phi) = m_1^2 \phi_1^2 + m_2^2 \phi_2^2 + 2m_3^2 \phi_1 \phi_2 + \frac{g^2 + g'^2}{8} (\phi_1^2 - \phi_2^2)^2, \quad (288)$$

$$V_1(\phi, 0) = \sum_i \frac{n_i}{64\pi^2} m_i^4(\phi) \left[\log \frac{m_i^2(\phi)}{Q^2} - \frac{3}{2} \right], \quad (289)$$

$$\Delta V_1(\phi, T) = \frac{T^4}{2\pi^2} \left\{ \sum_i n_i J_i \left[\frac{m_i^2(\phi)}{T^2} \right] \right\}, \quad (290)$$

$$\Delta V_{\text{daisy}}(\phi, T) = -\frac{T}{12\pi} \sum_{i=\text{bosons}} n_i [\mathcal{M}_i^3(\phi, T) - m_i^3(\phi)]. \quad (291)$$

The masses $\mathcal{M}_i^2(\phi, T)$ are obtained from the $m_i^2(\phi)$ by adding the leading T -dependent self-energy contributions, which are proportional to T^2 . We recall that, in the gauge boson sector, only the longitudinal components (W_L, Z_L, γ_L) receive such contributions.

The relevant degrees of freedom for our calculation are: $n_t = -12$, $n_{\tilde{t}_1} = n_{\tilde{t}_2} = 6$, $n_W = 6$, $n_Z = 3$, $n_{W_L} = 2$, $n_{Z_L} = n_{\gamma_L} = 1$. The field-dependent top mass is $m_{\tilde{t}}^2(\phi) = h_t^2 \phi_2^2$. The entries of the field-dependent stop mass matrix are

$$m_{\tilde{t}_L}^2(\phi) = m_{Q_3}^2 + m_{\tilde{t}}^2(\phi) + D_{\tilde{t}_L}^2(\phi), \quad (292)$$

$$m_{\tilde{t}_R}^2(\phi) = m_{U_3}^2 + m_{\tilde{t}}^2(\phi) + D_{\tilde{t}_R}^2(\phi), \quad (293)$$

$$m_X^2(\phi) = h_t(A_t \phi_2 - \mu \phi_1), \quad (294)$$

where m_Q , m_U and A_t are soft supersymmetry-breaking mass parameters, μ is a superpotential Higgs mass term, and

$$D_{\tilde{t}_L}^2(\phi) = \left(\frac{1}{2} - \frac{2}{3} \sin^2 \theta_W \right) \frac{g^2 + g'^2}{2} (\phi_1^2 - \phi_2^2), \quad (295)$$

$$D_{\tilde{t}_R}^2(\phi) = \left(\frac{2}{3} \sin^2 \theta_W \right) \frac{g^2 + g'^2}{2} (\phi_1^2 - \phi_2^2) \quad (296)$$

are the D -term contributions. The field-dependent stop masses are then

$$m_{\tilde{t}_{1,2}}^2(\phi) = \frac{m_{\tilde{t}_L}^2(\phi) + m_{\tilde{t}_R}^2(\phi)}{2} \pm \sqrt{\left[\frac{m_{\tilde{t}_L}^2(\phi) - m_{\tilde{t}_R}^2(\phi)}{2}\right]^2 + [m_X^2(\phi)]^2}. \quad (297)$$

The corresponding effective T -dependent masses, $\mathcal{M}_{\tilde{t}_{1,2}}^2(\phi, T)$, are given by expressions identical to (297), apart from the replacement

$$m_{\tilde{t}_{L,R}}^2(\phi) \rightarrow \mathcal{M}_{\tilde{t}_{L,R}}^2(\phi, T) \equiv m_{\tilde{t}_{L,R}}^2(\phi) + \Pi_{\tilde{t}_{L,R}}^{\sim}(T). \quad (298)$$

The $\Pi_{\tilde{t}_{L,R}}^{\sim}(T)$ are the leading parts of the T -dependent self-energies of $\tilde{t}_{L,R}$,

$$\Pi_{\tilde{t}_L}^{\sim}(T) = \frac{4}{9}g_s^2T^2 + \frac{1}{4}g^2T^2 + \frac{1}{108}g'^2T^2 + \frac{1}{6}h_t^2T^2, \quad (299)$$

$$\Pi_{\tilde{t}_R}^{\sim}(T) = \frac{4}{9}g_s^2T^2 + \frac{4}{27}g'^2T^2 + \frac{1}{3}h_t^2T^2, \quad (300)$$

where g_s is the strong gauge coupling constant. Only loops of gauge bosons, Higgs bosons and third generation squarks have been included, implicitly assuming that all remaining supersymmetric particles are heavy and decouple.

We shall work in the limit in which the left handed stop is heavy, $m_Q \gtrsim 500$ GeV. In this limit, the supersymmetric corrections to the precision electroweak parameter $\Delta\rho$ become small and hence, this allows a good fit to the electroweak precision data coming from LEP and SLD. Lower values of m_Q make the phase transition stronger and we are hence taking a conservative assumption from the point of view of defining the region consistent with electroweak baryogenesis. The left handed stop decouples at finite temperature, but, at zero temperature, it sets the scale of the Higgs masses as a function of $\tan\beta$. For right-handed stop masses below, or of order of, the top quark mass, and for large values of the CP-odd Higgs mass, $m_A \gg M_Z$, the one-loop improved Higgs effective potential admits a high temperature expansion,

$$V_0 + V_1 = -\frac{m^2(T)}{2}\phi^2 - T \left[E_{\text{SM}} \phi^3 + (2N_c) \frac{\left(m_{\tilde{t}}^2 + \Pi_{\tilde{t}_R}^{\sim}(T)\right)^{3/2}}{12\pi} \right] + \frac{\lambda(T)}{8}\phi^4 + \dots \quad (301)$$

where $N_c = 3$ is the number of colours and E_{SM} is the cubic term coefficient in the Standard Model case.

Within our approximation, the lightest stop mass is approximately given by

$$m_t^2 \simeq m_U^2 + 0.15M_Z^2 \cos 2\beta + m_t^2 \left(1 - \frac{\tilde{A}_t^2}{m_Q^2}\right) \quad (302)$$

where $\tilde{A}_t = A_t - \mu/\tan\beta$ is the stop mixing parameter. As was observed in Ref. ⁶⁸, the phase transition strength is maximized for values of the soft breaking parameter $m_U^2 = -\Pi_{tR}(T)$, for which the coefficient of the cubic term in the effective potential,

$$E \simeq E_{\text{SM}} + \frac{h_t^3 \sin^3 \beta \left(1 - \tilde{A}_t^2/m_Q^2\right)^{3/2}}{4\sqrt{2}\pi}, \quad (303)$$

can be one order of magnitude larger than E_{SM} ⁶⁸. In principle, the above would allow a sufficiently strong first order phase transition for Higgs masses as large as 100 GeV. However, it was also noticed that such large negative values of m_U^2 may induce the presence of color breaking minima at zero or finite temperature ^{68,69}. Demanding the absence of such dangerous minima, the one loop analysis leads to an upper bound on the lightest CP-even Higgs mass of order 80 GeV. This bound was obtained for values of $\tilde{m}_U^2 = -m_U^2$ of order $(80 \text{ GeV})^2$.

The most important two loop corrections are of the form $\phi^2 \log(\phi)$ and, as said above, are induced by the Standard Model weak gauge bosons as well as by the stop and gluon loops ⁷⁰. It was recently noticed that the coefficient of these terms can be efficiently obtained by the study of the three dimensional running mass of the scalar top and Higgs fields in the dimensionally reduced theory at high temperatures ⁷¹. Equivalently, in a four dimensional computation of the MSSM Higgs effective potential with a heavy left-handed stop, we obtain ⁶⁸

$$V_2 \simeq \log \frac{\Lambda_H}{\phi} \quad (304)$$

$$\frac{\phi^2 T^2}{32\pi^2} \left[\frac{51}{16} g^2 - 3 \left[h_t^2 \sin^2 \beta \left(1 - \frac{\tilde{A}_t^2}{m_Q^2}\right) \right]^2 + 8g_s^2 h_t^2 \sin^2 \beta \left(1 - \frac{\tilde{A}_t^2}{m_Q^2}\right) \right]$$

where the first term comes from the Standard Model gauge boson-loop contributions, while the second and third terms come from the light supersymmetric particle loop contributions. The scale Λ_H depends on the finite corrections, which may be obtained by the expressions given in ⁷². As mentioned above, the two-loop corrections are very important and, as has been shown in Ref. ⁷⁰, they

can make the phase transition strongly first order even for $m_U \simeq 0$ ⁷². Concerning the validity of the perturbative expansion, the β -parameter, similarly to β_{SM} , (283), can be shown to be given by

$$\beta_{\text{MSSM}} \sim \frac{m_h^2}{m_t^2}, \quad (305)$$

which leads to a reliable perturbative expansion for a value of the Higgs mass enhanced, with respect to its Standard Model value, by a factor $\sim (m_t/m_h)^2$.

An analogous situation occurs in the U -direction ($U \equiv \tilde{t}_R$). The one-loop expression is approximately given by

$$V_0(U) + V_1(U, T) = (-\tilde{m}_U^2 + \gamma_U T^2) U^2 - T E_U U^3 + \frac{\lambda_U}{2} U^4, \quad (306)$$

where γ_U and E_U were given in⁷².

Analogous to the case of the field ϕ , the two loop corrections to the U -potential are dominated by gluon and stop loops and are approximately given by

$$V_2(U, T) = \frac{U^2 T^2}{16\pi^2} \left[\frac{100}{9} g_s^4 - 2h_t^2 \sin^2 \beta \left(1 - \frac{\tilde{A}_t^2}{m_Q^2} \right) \right] \log \left(\frac{\Lambda_U}{U} \right) \quad (307)$$

where, as in the Higgs case, the scale Λ_U may only be obtained after the finite corrections to the effective potential are computed⁷².

Once the effective potential in the ϕ and U directions are computed, one can study the strength of the electroweak phase transition, as well as the presence of potential color breaking minima. At one-loop, it was observed that requiring the stability of the physical vacuum at zero temperature was enough to assure the absolute stability of the potential at finite temperature. As has been first noticed in Ref.⁷¹, once two loop corrections are included, the situation is more complicated⁷².

At zero temperature the minimization of the effective potential for the fields ϕ and U shows that the true minima are located for vanishing values of one of the two fields. The two set of minima are connected through a family of saddle points for which both fields acquire non-vanishing values. Due to the nature of the high temperature corrections, we do not expect a modification of this conclusion at finite temperature.

Two parameters control the presence of color breaking minima: \tilde{m}_U^c , defined as the smallest value of \tilde{m}_U for which a color breaking minimum deeper than the electroweak breaking minimum is present at $T = 0$, and T_c^U , the critical temperature for the transition into a color breaking minimum in the

U -direction. The value of \tilde{m}_U^c may be obtained by analysing the effective potential for the field U at zero temperature, and it is approximately given by⁶⁸

$$\tilde{m}_U^c \simeq \left(\frac{m_H^2 v^2 g_s^2}{12} \right)^{1/4}. \quad (308)$$

Defining the critical temperature as that at which the potential at the symmetry preserving and broken minima are degenerate, four situations can happen in the comparison of the critical temperatures along the ϕ (T_c) and U (T_c^U) transitions: **a)** $T_c^U < T_c$; $\tilde{m}_U < \tilde{m}_U^c$; **b)** $T_c^U < T_c$; $\tilde{m}_U > \tilde{m}_U^c$; **c)** $T_c^U > T_c$; $\tilde{m}_U < \tilde{m}_U^c$; **d)** $T_c^U > T_c$; $\tilde{m}_U > \tilde{m}_U^c$.

In case a), as the universe cools down, a phase transition into a color preserving minimum occurs, which remains stable until $T = 0$. This situation, of absolute stability of the physical vacuum, is the most conservative requirement to obtain electroweak baryogenesis. In case b), at $T = 0$ the color breaking minimum is deeper than the physical one implying that the color preserving minimum becomes unstable for finite values of the temperature, with $T < T_c$. A physically acceptable situation may only occur if the lifetime of the physical vacuum is smaller than the age of the universe. We shall denote this situation as “metastability”. In case c), as the universe cools down, a color breaking minimum develops which, however, becomes metastable as the temperature approaches zero. A physically acceptable situation can only take place if a two step phase transition occurs, that is if the color breaking minimum has a lifetime lower than the age of the universe at some temperature $T < T_c$ ⁷¹. Finally, in case d) the color breaking minimum is absolutely stable and hence, the situation becomes physically unacceptable.

Figure 9 shows the region of parameter space consistent with a sufficiently strong phase transition for $\tilde{A}_t = 0, 200, 300$ GeV. For low values of the mixing, $\tilde{A}_t \lesssim 200$ GeV, case a) or c) may occur but, contrary to what happens at one-loop, case b) is not realized. For the case of no mixing, this result is in agreement with the analysis of⁷¹. The region of absolute stability of the physical vacuum for $\tilde{A}_t \simeq 0$ is bounded to values of the Higgs mass of order 95 GeV. There is a small region at the right of the solid line, in which a two-step phase transition may take place, for values of the parameters which would lead to $v/T < 1$ for $T = T_c$, but may evolve to larger values at some $T < T_c$ at which the second of the two step phase transition into the physical vacuum takes place. This region disappears for larger values of the stop mixing mass parameter. For values of the mixing parameter \tilde{A}_t between 200 GeV and 300 GeV, both situations, cases b) and c) may occur, depending on the value of $\tan\beta$. For large values of the stop mixing, $\tilde{A}_t > 300$ GeV, a two-step phase

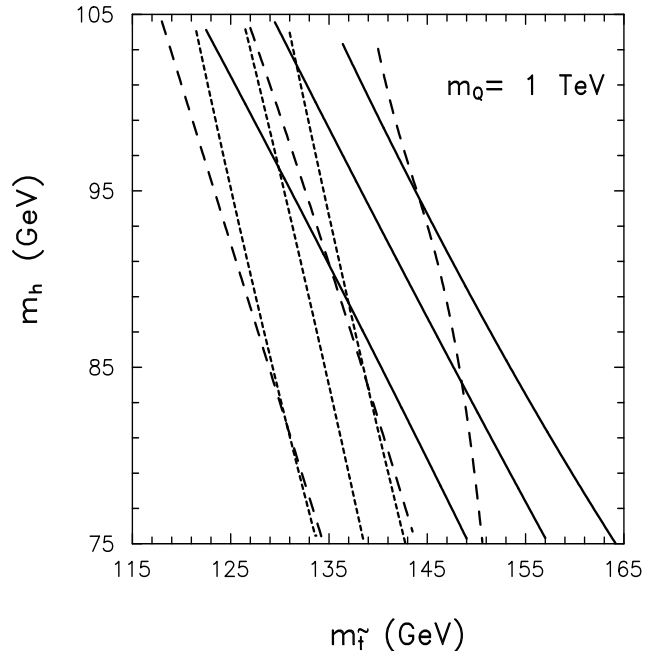


Figure 9: Values of m_h , $m_{\tilde{t}}$ for which $v(T_c)/T_c = 1$ (solid line), $T_c^U = T_c$ (dashed line), $\tilde{m}_U = \tilde{m}_U^c$ (short-dashed line), for $m_Q = 1$ TeV and $\tilde{A}_t = 0, 200, 300$ GeV. The region on the left of the solid line is consistent with a strongly first order phase transition. A two step phase transition may occur in the regions on the left of the dashed line, while on the left of the short-dashed line, the physical vacuum at $T = 0$ becomes metastable. The region on the left of both the dashed and short-dashed lines leads to a stable color breaking vacuum state at zero temperature and is hence physically unacceptable.

transition does not take place.

All together, and even demanding absolute stability of the physical vacuum, electroweak baryogenesis seems to work for a wide region of Higgs and stop mass values. Higgs masses between the present experimental limit, of about 90 GeV, and around 105 GeV are consistent with this scenario. Similarly, the running stop mass may vary from values of order 165 GeV (of the same order as the top quark mass one) and 100 GeV. Observe that, due to the influence of the D-terms, values of $m_{\tilde{t}} \simeq 165$ GeV, $\tilde{A}_t \simeq 0$ and $m_h \simeq 75$ GeV, are achieved for small positive values of m_U . Also observe that for lower values of m_Q the phase transition may become more strongly first order and slightly larger values of the stop masses may be obtained. Remind that these results are

based on the two-loop improved effective potential. Recent non-perturbative calculations⁷³ confirm the validity of these perturbative results.

References

1. W. Heisenberg and H. Euler, *Z. Phys.* **98** (1936) 714; J. Schwinger, *Phys. Rev.* **82** (1951) 664.
2. J. Goldstone, A. Salam and S. Weinberg, *Phys. Rev.* **127** (1962) 965; G. Jona-Lasinio, *Nuovo Cimento* **34** (1964) 1790.
3. S. Coleman and E. Weinberg, *Phys. Rev.* **D7** (1973) 1888.
4. R. Jackiw, *Phys. Rev.* **D9** (1974) 1686.
5. J. Iliopoulos, C. Itzykson and A. Martin, *Rev. Mod. Phys.* **47** (1975) 165.
6. J.D. Bjorken and S.D. Drell, *Relativistic Quantum Mechanics* (McGraw-Hill, 1964); *Relativistic Quantum Fields* (McGraw-Hill, 1965).
7. I.S. Gradshteyn and I.M. Ryzhik, *Table of Integrals Series and Products* (Academic Press, 1965).
8. G. t'Hooft and M. Veltman, *Nucl. Phys.* **B44** (1972) 189; C.G. Bollini and J.J. Giambiagi, *Phys. Lett.* **B40** (1972) 366; J.F. Ashmore, *Nuovo Cimento Letters* **4** (1972) 289.
9. G. t'Hooft and M. Veltman, *Nucl. Phys.* **B61** (1973) 455; W.A. Bardeen, A.J. Buras, D.W. Duke and T. Muta, *Phys. Rev.* **D18** (1978) 3998.
10. See, e.g.: J. Collins, *Renormalization* (Cambridge University Press, 1984).
11. W. Siegel, *Phys. Lett.* **B84** (1979) 193.
12. G.W. Anderson and L.J. Hall, *Phys. Rev.* **D45** (1992) 2685.
13. B. Kastening, *Phys. Lett.* **B283** (1992) 287; M. Bando, T. Kugo, N. Maekawa and H. Nakano, *Phys. Lett.* **B301** (1993) 83; C. Ford, D.R.T. Jones, P.W. Stephenson and M.B. Einhorn, *Nucl. Phys.* **B395** (1993) 17.
14. A. Casas, J.R. Espinosa, M. Quirós and A. Riotto, *Nucl. Phys.* **B436** (1995) 3.
15. L. Dolan and R. Jackiw, *Phys. Rev.* **D9** (1974) 3320.
16. S. Weinberg, *Phys. Rev.* **D9** (1974) 3357.
17. R.H. Brandenberger, *Rev. Mod. Phys.* **57** (1985) 1.
18. N.P. Landsman and Ch.G. van Weert, *Phys. Rep.* **145** (1987) 141.
19. M. Quirós, *Helv. Phys. Acta* **67** (1994) 451.
20. J.I. Kapusta, *Finite-temperature field theory* (Cambridge University Press, 1989).
21. R. Kubo, *J. Phys. Soc. Japan* **12** (1957) 570; P.C. Martin and J.

- Schwinger, *Phys. Rev.* **115** (1959) 1342.
22. T. Matsubara, *Prog. Theor. Phys.* **14** (1955) 351.
 23. H. Matsumoto, Y. Nakano, H. Umezawa, F. Mancini and M. Marinaro, *Prog. Theor. Phys.* **70** (1983) 599; H. Matsumoto, Y. Nakano and H. Umezawa, *J. Math. Phys.* **25** (1984) 3076.
 24. L.V. Keldish, *Sov. Phys. JETP* **20** (1964) 1018.
 25. T.S. Evans, *Phys. Rev.* **D47** (1993) R4196; T. Altherr, CERN preprint, CERN-TH.6942/93.
 26. R. Kobes, *Phys. Rev.* **D42** (1990) 562 and *Phys. Rev. Lett.* **67** (1991) 1384; T.S. Evans, *Phys. Lett.* **B249** (1990) 286, *Phys. Lett.* **B252** (1990) 108, *Nucl. Phys.* **B371** (1992) 340; P. Aurenche and T. Becher-rawy, *Nucl. Phys.* **B379** (1992) 259; M.A. van Eijck and Ch. G. van Weert, *Phys. Lett.* **B278** (1992) 305.
 27. D.A. Kirzhnits, *JETP Lett.* **15** (1972) 529.
 28. D.A. Kirzhnits and A.D. Linde, *Phys. Lett.* **42B** (1972) 471; D.A. Kirzhnits and A.D. Linde, *JETP* **40** (1974) 628; D.A. Kirzhnits and A.D. Linde, *Ann. Phys.* **101** (1976) 195.
 29. A.D. Linde, *Rep. Prog. Phys.* **42** (1979) 389; A.D. Linde, *Phys. Lett.* **99B** (1981) 391; A.D. Linde, *Phys. Lett.* **99B** (1981) 391; A.D. Linde, *Particle Physics and Inflationary Cosmology* (Harwood, Chur, Switzerland, 1990).
 30. A.D. Linde, *Phys. Lett.* **B108** (1982) 389; A. Albrecht and P.J. Steinhardt, *Phys. Rev. Lett.* **48** (1982) 1226.
 31. M. Dine, R.G. Leigh, P. Huet, A. Linde and D. Linde, *Phys. Lett.* **B283** (1992) 319; *Phys. Rev.* **D46** (1992) 550.
 32. S. Coleman, *Phys. Rev.* **D15** (1977) 2929.
 33. C.G. Callan and S. Coleman, *Phys. Rev.* **D16** (1977) 1762.
 34. S. Coleman and F. De Luccia, *Phys. Rev.* **D21** (1980) 3305.
 35. A.D. Linde, *Phys. Lett.* **70B** (1977) 306; **100B** (1981) 37; *Nucl. Phys.* **B216** (1983) 421.
 36. L. McLerran, M. Shaposhnikov, N. Turok and M. Voloshin, *Phys. Lett.* **B256** (1991) 451.
 37. M. Dine, P. Huet and R. Singleton Jr., *Nucl. Phys.* **B375** (1992) 625.
 38. J.M. Moreno, M. Quirós and M. Seco, *Nucl. Phys.* **B526** (1998) 489.
 39. E.W. Kolb and M.S. Turner, *The Early Universe* (Addison-Wesley, 1990).
 40. A.D. Sakharov, *Zh. Eksp. Teor. Fiz. Pis'ma* **5** (1967) 32; *JETP Lett.* **91B** (1967) 24.
 41. Particle Data Group, Review of Particle Properties, *Eur. Phys. J.* **C3** (1998) 1.
 42. E.W. Kolb and S. Wolfram, *Nucl. Phys.* **B172** (1980) 224; *Phys. Lett.*

- B91** (1980) 217.
43. V.A. Kuzmin, V.A. Rubakov and M.E. Shaposhnikov, *Phys. Lett.* **B155** (1985) 36; *Phys. Lett.* **B191** (1987) 171.
 44. A.G. Cohen, D.B. Kaplan and A.E. Nelson, *Annu. Rev. Nucl. Part. Sci.* **43** (1993) 27.
 45. G. t' Hooft, *Phys. Rev. Lett.* **37** (1976) 8; *Phys. Rev.* **D14** (1976) 3432.
 46. M. Kobayashi and M. Maskawa, *Prog. Theor. Phys.* **49** (1973) 652.
 47. N.S. Manton, *Phys. Rev.* **D28** (1983) 2019; F.R. Klinkhamer and N.S. Manton, *Phys. Rev.* **D30** (1984) 2212.
 48. J. Kunz, B. Kleihaus and Y. Brihaye, *Phys. Rev.* **D46** (1992) 3587.
 49. Y. Brihaye and J. Kunz, *Phys. Rev.* **D48** (1993) 3884.
 50. J.M. Moreno, D.H. Oaknin and M. Quirós, [hep-ph/9605387], *Nucl. Phys.* **B483** (1997) 267.
 51. P. Arnold and L. McLerran, *Phys. Rev.* **D36** (1987) 581; S.Yu. Khlebnikov and M.E. Shaposhnikov, *Nucl. Phys.* **B308** (1988) 885.
 52. J. Ambjorn, M. Laursen and M. Shaposhnikov, *Phys. Lett.* **B197** (1989)49; J. Ambjorn, T. Askaard, H. Porter and M. Shaposhnikov, *Phys. Lett.* **B244** (1990) 479; *Nucl. Phys.* **B353** (1991) 346; J. Ambjorn and K. Farakos, *Phys. Lett.* **B294** (1992) 248; J. Ambjorn and A. Krasnitz, *Phys. Lett.* **B362** (1995) 97.
 53. P. Arnold, D. Son and L.G. Yaffe, *Phys. Rev.* **D55** (1997) 6264; hep-ph/9810216; hep-ph/9810217; G.D. Moore, *Phys. Rev.* **D59** (1999) 014503; hep-ph/9810313; D. Bodeker, *Phys. Lett.* **B426** (1998) 351; hep-ph/9810265.
 54. L. Carson, Xu Li, L. McLerran and R.-T. Wang, *Phys. Rev.* **D42** (1990) 2127.
 55. M.E. Shaposhnikov, *Nucl. Phys.* **B287** (1987) 757; *Nucl. Phys.* **B299** (1988) 797; A.I. Bochkarev and M.E. Shaposhnikov, *Mod. Phys. Lett* **A2** (1987) 417.
 56. A.I. Bochkarev, S.V. Kuzmin and M.E. Shaposhnikov, *Phys. Rev.* **D43** (1991) 369.
 57. P. Fendley, *Phys. Lett.* **B196** (1987) 175.
 58. J.R. Espinosa, M. Quirós and F. Zwirner, *Phys. Lett.* **B291** (1992) 115.
 59. D.J. Gross, R.D. Pisarski and L.G. Yaffe, *Rev. Mod. Phys.* **53** (1981) 43.
 60. R.R. Parwani, *Phys. Rev.* **D45** (1992) 4695.
 61. P. Arnold and O. Espinosa, *Phys. Rev.* **D47** (1993) 3546.
 62. M.E. Carrington, *Phys. Rev.* **D45** (1992) 2933.
 63. K. Jansen, *Nucl. Phys. (Proc. Supl.)* **B47** (1996) 196 [hep-lat/9509018].
 64. A.G. Cohen and A.E. Nelson, *Phys. Lett.* **B297** (1992) 111.

65. J.R. Espinosa, M. Quiros and F. Zwirner, *Phys. Lett.* **B307** (1993) 106.
66. A. Brignole, J.R. Espinosa, M. Quiros and F. Zwirner, *Phys. Lett.* **B324** (1994) 181.
67. G.F. Giudice, *Phys. Rev.* **D45** (1992) 3177; S. Myint, *Phys. Lett.* **B287** (1992) 325.
68. M. Carena, M. Quiros and C.E.M. Wagner, *Phys. Lett.* **B380** (1996) 81
69. M. Carena and C.E.M. Wagner, *Nucl. Phys.* **B452** (1995) 45
70. J.R. Espinosa, *Nucl. Phys.* **B475** (1996) 273; B. de Carlos and J.R. Espinosa, [hep-ph/9703212], *Nucl. Phys.* **B503** (1997) 24.
71. D. Bodeker, P. John, M. Laine and M.G. Schmidt, *Nucl. Phys.* **B497** (1997) 387
72. M. Carena, M. Quiros and C.E.M. Wagner, [hep-ph/9710401] *Nucl. Phys.* **B524** (1998) 3.
73. M. Laine and K. Rummukainen, *Phys. Rev. Lett.* **80** (1998) 5259; *Nucl. Phys.* **B535** (1998) 423.